IL NUOVO CIMENTO

rivista internazionale di fisica

fondata a Pisa nel 1855 da C. MATTEUCCI e R. PIRIA
dal 1897 Organo della Società Italiana di Fisica

pubblicata
sotto gli auspici del Consiglio Nazionale delle Ricerche

a cura del Direttore
RENATO ANGELO RICCI
Presidente della Società

e dei Vicedirettori
R. R. GATTO e P. PICCHI

La collaborazione alla *Rivista del Nuovo Cimento* è esclusivamente su invito. I lavori possono essere scritti in francese, inglese, italiano, spagnolo o tedesco.

Si prega vivamente d'inviare i lavori destinati alla pubblicazione, in duplice copia, direttamente al **Direttore del Nuovo Cimento, via degli Andalò, 2 - 40124 Bologna**. Ciascuna copia, scritta a macchina su un solo lato del foglio, deve essere corredata di disegni, fotografie e bibliografia con i nomi e le iniziali di tutti gli autori; una serie di disegni originali in inchiostro di China su carta da lucidi deve essere allegata alle copie del lavoro; le eventuali fotografie devono essere stampate su carta bianca lucida pesante. Non si accettano manoscritti in una sola copia od incompleti. I manoscritti non si restituiscono.

Di regola le bozze sono inviate agli autori una sola volta, salvo che siano state esplicitamente richieste seconde bozze.

Gli autori non hanno spese di pubblicazione, salvo quelle per le correzioni dovute ad insufficienze del manoscritto inviato per la pubblicazione, modifiche del testo originario, modifiche o rifacimenti di figure, ecc.

Gli estratti (eventualmente con copertine stampate e montate apposta) possono essere forniti a richiesta secondo la tariffa che la Redazione comunicherà agl'interessati. L'importo degli estratti assieme a quello per le correzioni straordinarie sarà fatturato dall'**Editrice Compositori, via Stalingrado, 97/2 - 40128 Bologna**.

Norme piú dettagliate si trovano nella «Guida per gli Autori», che viene inviata gratuitamente su richiesta.

Contribution to *Rivista del Nuovo Cimento* is by invitation only. Papers may be written in English, French, German, Italian or Spanish.

Manuscripts submitted for publication should be sent in triplicate and only to **The Director of Il Nuovo Cimento, via degli Andalò, 2 - I 40124 Bologna (Italy)**. Each copy, typewritten on one side of the sheets only, must be complete with drawings, photographs and references with the names and initials of all the authors; a set of original drawings in India ink on tracing paper must be enclosed with the copies of the manuscript; photographs must be on heavy-weight glossy white paper. Manuscripts either in single copies or incomplete will not be accepted. Manuscripts will not be returned.

Proofs will be sent only once unless second proofs are specifically requested for by the author.

Authors will be charged only for corrections due to lack of clarity of the manuscript submitted, modifications to the original text, modifications or remaking of figures, etc.

Reprints as well as covers printed to order may be supplied on payment. The Editorial Office will give the corresponding prices on request. The cost of the reprints and the charges for corrections will be invoiced by **Editrice Compositori, via Stalingrado, 97/2 - I 40128 Bologna (Italy)**.

Further details are contained in the «Guide for the Authors», which will be sent free on request.

Direzione e Redazione Via degli Andalò, 2 40124 Bologna

A. CRISANTI, M. FALCIONI, G. PALADIN and A. VULPIANI

Lagrangian Chaos: Transport, Mixing and Diffusion in Fluids.

RIVISTA DEL NUOVO CIMENTO VOL. 14, N. 12 1991

Lagrangian Chaos: Transport, Mixing and Diffusion in Fluids.

A. CRISANTI, M. FALCIONI and A. VULPIANI

Dipartimento di Fisica - Università di Roma «La Sapienza»
Piazzale Aldo Moro 2 - I-00185 Roma - Italy

G. PALADIN

Dipartimento di Fisica - Università dell'Aquila
Via Vetoio - I-67100 Coppito - L'Aquila - Italy

(ricevuto il 19 Novembre 1991)

1. – Introduction.

The hydrodynamic equations of motion can be studied in two different approaches. Either one deals at any time with velocity, pressure and density fields in the space domain covered by the fluid, or one deals with the trajectory

of each fluid particle. The two approaches are usually designed as «Eulerian» and «Lagrangian», although both of them are due to Euler [L45].

The two points of view are in principle equivalent. Indeed, if we denote by $\boldsymbol{u}(\boldsymbol{x}, t)$ the Eulerian velocity field, then the motion of a fluid particle initially located at $\boldsymbol{x}(0)$ is determined by the differential equation

$$\frac{\mathrm{d}\boldsymbol{x}}{\mathrm{d}t} = \boldsymbol{u}(\boldsymbol{x}, t) \tag{1.1}$$

with the initial condition $\boldsymbol{x}(0)$. If the solution of (1.1) has a sensitive dependence on initial conditions, and initially nearby trajectories diverge exponentially fast, one speaks of *Lagrangian chaos or Lagrangian turbulence*.

However, in spite of the simple formal relation between Eulerian and Lagrangian approach, it is difficult to extract information on one description starting from the other. For instance, there are situations where the velocity field is regular — *i.e.* absence of Eulerian chaos — but the corresponding motion of fluid particles is chaotic [H66].

The motion of a fluid particle in a given velocity field $\boldsymbol{u}(\boldsymbol{x}, t)$ is given by the dynamical system (1.1), which is conservative for an incompressible fluid, that is, by the continuity equation, for a solenoidal velocity field

$$\nabla \cdot \boldsymbol{u} = 0 . \tag{1.2}$$

In two dimensions, the constraint (1.2) is automatically satisfied assuming

$$u_1 = \frac{\partial \psi}{\partial x_2}, \qquad u_2 = -\frac{\partial \psi}{\partial x_1}, \tag{1.3}$$

where $\psi(\boldsymbol{x}, t)$ is called *stream function*, and $\boldsymbol{x} = (x_1, x_2)$. Inserting (1.3) into (1.1) the evolution equations become

$$\dot{x}_1 = \frac{\partial \psi}{\partial x_2}, \qquad \dot{x}_2 = -\frac{\partial \psi}{\partial x_1}. \tag{1.4}$$

Formally (1.4) is a Hamiltonian system with the Hamiltonian given by the stream function ψ.

Equation (1.1) also describes the motion of test particles, for example a powder embedded in the fluid, under the condition that the particles are small enough not to perturb the velocity field, but also large enough not to perform a Brownian motion. Particles of this type are the tracers used for flow visualization in fluid mechanics experiments [T88]. This subject will be discussed in more details in sect. **5**.

The understanding of Lagrangian dynamics is a central point for the problem of quantities passively driven by the flow, *e.g.* the temperature under certain conditions, the theory of mixing and fast dynamo effects [M83, OLRS88]. The evolution of a passive scalar field $\Theta(\boldsymbol{x}, t)$ is given by

$$\partial_t \Theta + (\boldsymbol{u} \cdot \nabla)\Theta = \chi_\theta \nabla^2 \Theta , \tag{1.5}$$

where χ_θ is the molecular field diffusion coefficient. If $\chi_\theta = 0$, it is easy to realize that (1.5) is equivalent to (1.1). In fact, we can write

$$\Theta(\boldsymbol{x}, t) = \Theta_0(\boldsymbol{T}^{-t}\boldsymbol{x}), \tag{1.6}$$

where $\Theta_0(\boldsymbol{x}) = \Theta(\boldsymbol{x}, t = 0)$ and $\boldsymbol{T}$ is the formal evolution operator of (1.1),

$$\boldsymbol{x}(t) = \boldsymbol{T}^t \boldsymbol{x}(0). \tag{1.7}$$

Taking into account the molecular diffusion χ_θ, one has [C43] that (1.5) is the Fokker-Planck equation of the Langeving equation

$$\frac{\mathrm{d}\boldsymbol{x}}{\mathrm{d}t} = \boldsymbol{u}(\boldsymbol{x}, t) + \boldsymbol{\eta}(t), \tag{1.8}$$

where $\boldsymbol{\eta}$ is a Gaussian process with zero mean and

$$\langle \eta_i(t)\eta_j(t')\rangle = 2\chi_\theta \delta_{ij}\delta(t - t').$$

It is clear that the Eulerian approach (1.5) and the Lagrangian one (1.8) are completely equivalent.

The presence of Lagrangian chaos, even in the absence of Eulerian chaos, indicates that some gross properties of mixing and diffusion are not strongly related to the presence of the diffusive term $\chi_\theta \nabla^2 \Theta$. Therefore, although the two approaches are equivalent, in many cases the Lagrangian description permits a better understanding of the physics [O89, O90].

The so-called kinematic dynamo is another problem where the role of Lagrangian chaos is important; see for instance [GF84, B86, BC87, FO88, FPV89]. With appropriate approximations the behaviour of a magnetic field $\boldsymbol{B}(\boldsymbol{x}, t)$ can be described by the following equations:

$$\begin{cases} \partial_t \boldsymbol{B} + (\boldsymbol{u}\cdot\nabla)\boldsymbol{B} = (\boldsymbol{B}\cdot\nabla)\boldsymbol{u} + \chi_B \nabla^2 \boldsymbol{B}, \\ \nabla\cdot\boldsymbol{B} = 0, \end{cases} \tag{1.9}$$

where χ_B is the magnetic-diffusion coefficient of the fluid. In the limit $\chi_B \to 0$, it is possible to see that there is a connection between the kinematic dynamo equation and the dynamical system (1.1).

Consider the equation which masters the time evolution of the «distance» vector $\boldsymbol{R} = \boldsymbol{x}^{(2)} - \boldsymbol{x}^{(1)}$ between two particles located at $\boldsymbol{x}^{(1)}$ and $\boldsymbol{x}^{(2)}$, respectively. In the limit $|\boldsymbol{R}| \to 0$ the evolution equation for $\boldsymbol{R}$ can be obtained by linearizing (1.1) around the trajectory $\boldsymbol{x}(t) = \boldsymbol{x}^{(1)}(t)$. This leads to the equation for the tangent vector $\boldsymbol{z} = \lim_{|R|\to 0}(\boldsymbol{x}^{(1)} - \boldsymbol{x}^{(2)})$,

$$\frac{\mathrm{d}z_i}{\mathrm{d}t} = \sum_{j=1}^{d} \left.\frac{\partial u_i}{\partial x_j}\right|_{x(t)} z_j. \tag{1.10}$$

The Lagrangian time derivative can be expressed in the form $\mathrm{d}/\mathrm{d}t = \partial_t + (\boldsymbol{u}\cdot\nabla)$, so that (1.9) with $\chi_B = 0$ is formally equal to (1.10). The behaviour of the

magnetic field is governed by two properties of (1.1), *i.e.* the trajectories of the fluid particles and the growth rate of the tangent vector — that is of the separation of particle pairs. However, the role of the term $\chi_B \nabla^2 \boldsymbol{B}$ is highly nontrivial. This point is stressed in sect. **4**.

In this review we discuss the role of Lagrangian chaos in mixing, transport and diffusion properties of fluids, using ideas and techniques borrowed by the theory of chaotic dynamical systems. Our main interest stems from the physical applications, so that most of technical details on the methods used will be left to sect. **6**. The review is organized as follows.

In sect. **2** we discuss some examples of Lagrangian chaos which show the strong relation between mixing mechanisms and properties of the dynamical system (1.1).

Section **3** is devoted to the connection between Lagrangian chaos and Eulerian properties of the velocity field. We indicate, in particular, a possible route for the onset of Lagrangian chaos in two-dimensional fluids.

In sect. **4**, we study the small-scale structure of passive scalars in incompressible fluids. We show that the classical Batchelor law (which gives a k^{-1} scaling for the power spectrum of the passive scalar in a suitable range of wave numbers k) is strictly related to the Lagrangian chaos and, hence, it is also valid for fluids which are not turbulent in the Eulerian sense. We also discuss the very irregular small-scale structure of magnetic field due to the intermittency of the dynamical system (1.1). Finally, using some results obtained in the study of Lagrangian chaos, we comment on the temporal range of validity of the classical limit of quantum mechanics.

In sect. **5** we discuss the diffusive properties of (1.1) and (1.8). In general they are very sensitive to the details of the structure of the velocity field and to the combined effects of that structure and molecular diffusion.

Section **6** reports, for the sake of self-consistency, some technical aspects and methods of dynamical systems which are relevant for the comprehension of Lagrangian chaos in fluids.

2. – Lagrangian chaos.

In this section we report some examples of Lagrangian chaos in regular velocity fields; moreover we discuss the problem of the stretching of material lines and surfaces in terms of Lyapunov exponents. The presence of Lagrangian chaos in regular velocity fields may appear as a paradox, but it has not to be considered too surprising. Since (1.1) is a nonlinear dynamical system, in general one can expect that a chaotic behaviour arises for time-dependent velocity fields in two dimensions ($2d$), or even for stationary velocity fields in three dimensions ($3d$).

2·1. *Examples of Lagrangian chaos.* – As first case, we consider the following $3d$ stationary velocity field:

$$\boldsymbol{u}(\boldsymbol{x}) \equiv (A \sin z + C \cos y,\ B \sin x + A \cos z,\ C \sin y + B \cos x)\,, \tag{2.1}$$

where A, B and C are nonzero real parameters. According to (2.1) the

dynamical system associated with the fluid particle motion is

$$\begin{cases} \dfrac{\mathrm{d}x}{\mathrm{d}t} = A \sin z + C \cos y\,, \\ \dfrac{\mathrm{d}y}{\mathrm{d}t} = B \sin x + A \cos z\,, \\ \dfrac{\mathrm{d}z}{\mathrm{d}t} = C \sin y + B \cos x\,. \end{cases} \tag{2.2}$$

Because of the incompressibility condition $\nabla \cdot \boldsymbol{u} = 0$, the evolution $\boldsymbol{x}(0) \rightarrow \boldsymbol{x}(t)$, given by the differential equations (2.2), defines a volume-preserving dynamical system.

Arnold [A65] argued that (2.2) is a good candidate for chaotic motion. Let us briefly repeat the argument. In a steady-state solution of the $3d$ Euler equation one has

$$\begin{cases} \nabla \cdot \boldsymbol{u} = 0\,, \\ \boldsymbol{u} \times (\nabla \times \boldsymbol{u}) = \nabla \alpha\,, \\ \alpha = \dfrac{P}{\rho} + \dfrac{\boldsymbol{u}^2}{2}\,, \end{cases} \tag{2.3}$$

where P is the pressure and ρ the density. As a consequence of the Bernoulli theorem [LL87], $\alpha(\boldsymbol{x})$ is constant along a streamline — that is a trajectory of the system $\mathrm{d}\boldsymbol{x}/\mathrm{d}t = \boldsymbol{u}(\boldsymbol{x})$. One can easily realize that a chaotic motion may appear only if $\alpha(\boldsymbol{x})$ is constant (*viz.* $\nabla\alpha(\boldsymbol{x}) = 0$) in a region of the space. Otherwise the trajectory would be confined on a $2d$ surface $\alpha(\boldsymbol{x}) =$ constant, where the motion must be regular for general arguments (Bendixson-Poincaré theorem [A72]). In order to have this constraint, one has to impose the Beltrami properties

$$\nabla \times \boldsymbol{u} = \gamma(\boldsymbol{x})\,\boldsymbol{u}(\boldsymbol{x})\,, \qquad \boldsymbol{u}(\boldsymbol{x}) \cdot \nabla\gamma(\boldsymbol{x}) = 0\,. \tag{2.4}$$

The $\boldsymbol{u}(\boldsymbol{x})$ given by (2.1) is a simple case of velocity field with the Beltrami properties (in this case $\gamma(\boldsymbol{x}) =$ constant). It is possible to show [GF87] that (2.1) is the unique stable solution of the Navier-Stokes equations

$$\begin{cases} \partial_t \boldsymbol{u} + (\boldsymbol{u} \cdot \nabla)\,\boldsymbol{u} = \nu\nabla^2\boldsymbol{u} - \dfrac{1}{\rho}\nabla P + \boldsymbol{f}\,, \\ \nabla \cdot \boldsymbol{u} = 0\,, \end{cases} \tag{2.5}$$

for large ν and with the forcing

$$\boldsymbol{f} \equiv \nu(A \sin z + C \cos y,\ B \sin x + A \cos z,\ C \sin y + B \cos x)\,.$$

If the Eulerian evolution of the velocity field is not given by the Euler

equation, the Beltrami properties are not mandatory for chaos. For example, Arter [A83] found a chaotic behaviour in steady Rayleigh-Bénard convection, where the Eulerian evolution is ruled by the Boussinesq model.

Equation (2.2) was independently introduced by Childress [C70] as a model for kinematic dynamos, and now these flows are usually indicated as ABC flows (for Arnold, Beltrami, Childress). Numerical experiments by Hénon [H66] provided evidence that they are chaotic for special values of the parameters A, B, and C. An extensive numerical and analytical study of the ABC model can be found in [DFGHMS86].

Without entering in a detailed analysis, we show in fig. 1 the Poincaré section at $z = 0$ of several trajectories. The ordered motions and the chaotic ones are well evident: a situation recalling the features of nonintegrable Hamiltonian systems with two degrees of freedom.

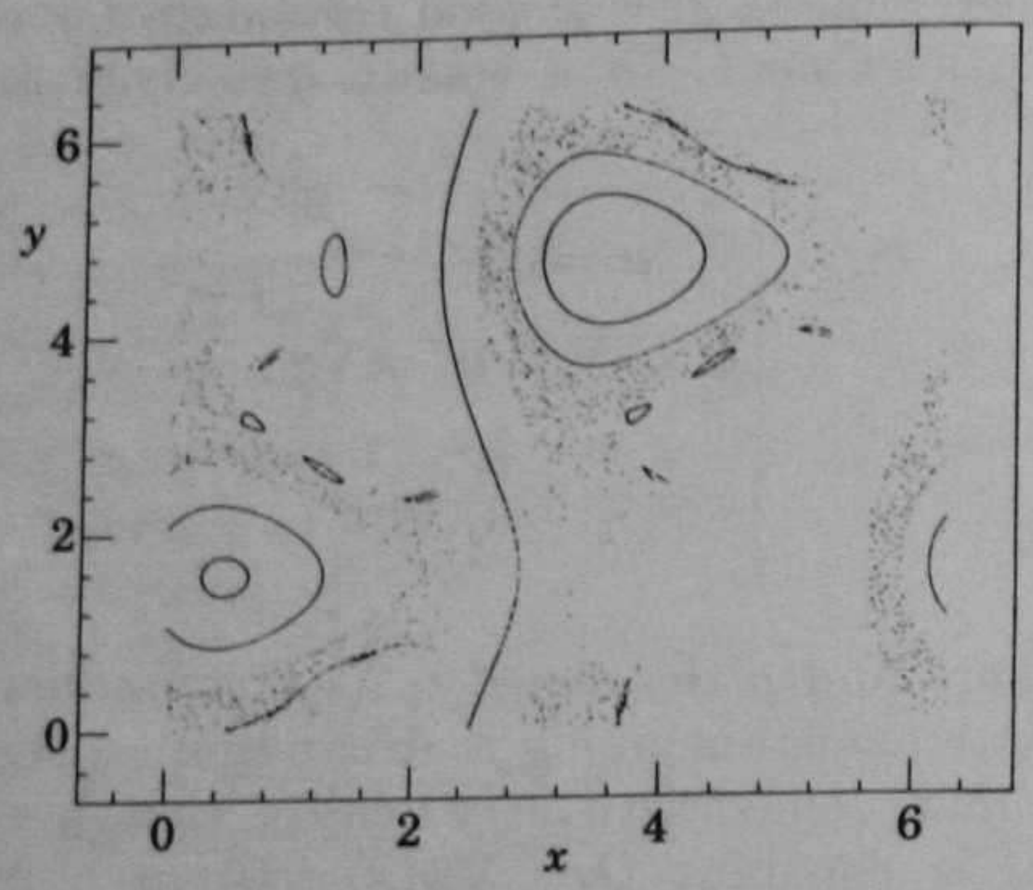

Fig. 1. – Intersections with the Poincaré section, plane $z = 0$, of eigth trajectories of the ABC flow, eq. (2.2) with parameters $A = 2.0$, $B = 1.70$, $C = 1.50$.

For two-dimensional incompressible and stationary flows, the stream function ψ does not depend on the time, so the motion of fluid particles is given by a time-independent Hamiltonian system with one degree of freedom, and it is impossible to have a chaotic motion. However, for explicit time-dependent ψ the system (1.4) can exhibit chaotic motion. For example many authors studied the $2d$ chaotic advection in Stokes flows [AB86, CCTT87] (*i.e.* in a fluid between two eccentric cylinders which rotate with a given time-dependent angular velocity) or in a simple model which provides an idealization of a stirred tank [A84].

We briefly discuss another example of chaotic advection [LS89] associated with a mode of free oscillation for a layer of water of depth D in a rectangular basin. In the linear inviscid shallow-water approximation, and considering only two modes in the Fourier expansion of the velocity field, one can write

$$\boldsymbol{u} \equiv ((a + b\cos(2t))\sin x \cos y,\ -(a - b\cos(2t))\cos x \sin y)\,, \tag{2.6}$$

where a convenient rescaling of lengths and time is used. The motion of fluid

particles is thus given by

$$\begin{cases} \dfrac{\mathrm{d}x}{\mathrm{d}t} = (a + b\cos(2t))\sin x\cos y\,, \\ \dfrac{\mathrm{d}y}{\mathrm{d}t} = -(a - b\cos(2t))\cos x\sin y\,. \end{cases} \tag{2.7}$$

Apart from the case $b = 0$, the velocity field (2.6) does not satisfy the incompressibility condition, so that (2.7) is not a Hamiltonian system. For $b = 0$ the dynamical system (2.7) is integrable and can be easily reduced to the ABC flow with $C = 0$ and $A = B$.

Also in the present case the Poincaré section, obtained by plotting the coordinates x and y at each period (*i.e.* at times $t = 0,\ \pi,\ 2\pi,\ \ldots$) allows us to visualize the regular and the chaotic motion; see fig. 2.

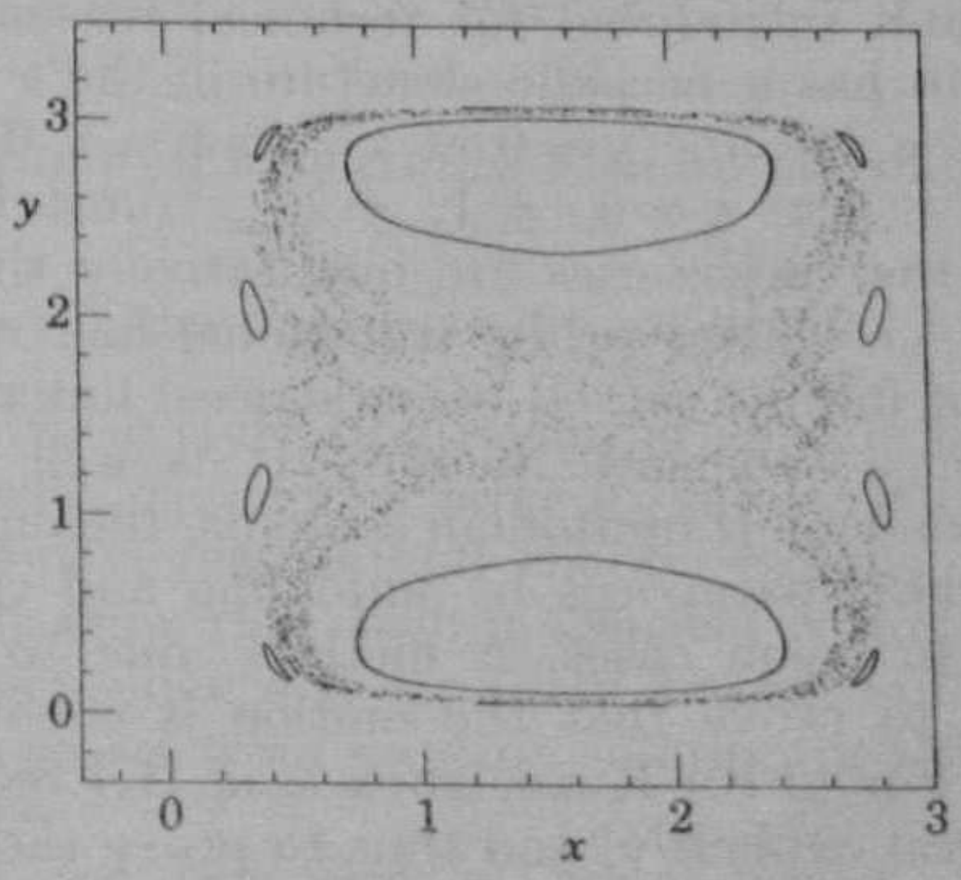

Fig. 2. – Iterations of the Poincaré map $\boldsymbol{x} = \boldsymbol{x}(nT)$, with $T = \pi$, of three trajectories of the flow (2.7), with parameters $a = 1.35$, $b = 1.15$.

We now give an example to emphasize one of the basic mechanisms for the chaotic advection in $2d$ incompressible flow [KRS83]. An exact solution of $2d$ Euler equation which mimics large-scale vortex structure is given by

$$\psi_0(x,\ y) = \frac{\Gamma}{2\pi}\ln\left(\cosh\frac{2\pi y}{l} - \alpha\cos\frac{2\pi x}{l}\right). \tag{2.8}$$

Here l indicates the period of the vortex series in the x-direction, and α describes the vorticity distribution: $\alpha = 0$ corresponds to a uniform distribution and $\alpha = 1$ gives a series of point vortices. In realistic situations one has rather concentrated vorticity distribution, so it is natural to assume $\alpha \lesssim 1$. We discuss the case $\alpha = 1$, although the qualitative results will be valid also for $\alpha < 1$. A realistic perturbation to the steady solution (2.8) is an external wave

propagating perpendicularly to the series, *i.e.*

$$\delta \boldsymbol{u} = (0,\ u_0 \sin (2ky - 2\omega t)) . \tag{2.9}$$

In the approximation of shear layer thickness smaller than the wavelength ($kl \ll 1$), and of small-wave amplitude ($\mu_0 = u_0/c \ll 1$, where $c = \omega/k$ is the wave velocity) the Lagrangian equations (1.1) become

$$\begin{cases} \dfrac{\mathrm{d}x}{\mathrm{d}t} = -h \dfrac{\sinh y}{\cosh y - \cos x}, \\ \dfrac{\mathrm{d}y}{\mathrm{d}t} = h \dfrac{\sin x}{\cosh y - \cos x} + 2\mu_0 y \dfrac{\omega h}{\Omega} \cos\left(\dfrac{2\omega h}{\Omega} t\right). \end{cases} \tag{2.10}$$

In (2.10) one uses dimensionless coordinates and time, $\Omega = \pi\Gamma/l^2$ and h is the dimensionless time unit introduced for technical reasons, see [KRS83]. Note that the system (2.10) has a periodic structure in the x-direction. For $\mu_0 = 0$ the fixed points are on the line $y = 0$ at $x = 2n\pi$, $n = 0, \pm 1, \pm 2, \ldots$ (stable points), and $x = (2n + 1)\pi$, $n = 0, \pm 1, \pm 2, \ldots$ (unstable points). It is not difficult to see that the trajectories are qualitatively similar to those of the nonlinear pendulum, *i.e.* closed orbits (rotations) and open ones (librations) separated by orbits of infinite period (separatrices) linking two unstable fixed points; see fig. 3 for a schematic picture. It is well known that in one-dimensional time-dependent Hamiltonian systems, the onset of chaos typically takes place around the separatrices by unfolding and crossing of stable and unstable manifolds. In some cases, a method, due to Melnikov [M63], see subsect. **6**·2, permits to prove that the motion is chaotic in a small region around a separatrix. For (2.10) Kuznetsova *et al.* [KRS83] were able to compute Melnikov's integral explicitly, and thus to prove the existence of Lagrangian chaos. Figure 4 illustrates, by means of a Poincaré section, the typical behaviour of the system at small value of the perturbative parameter μ_0:

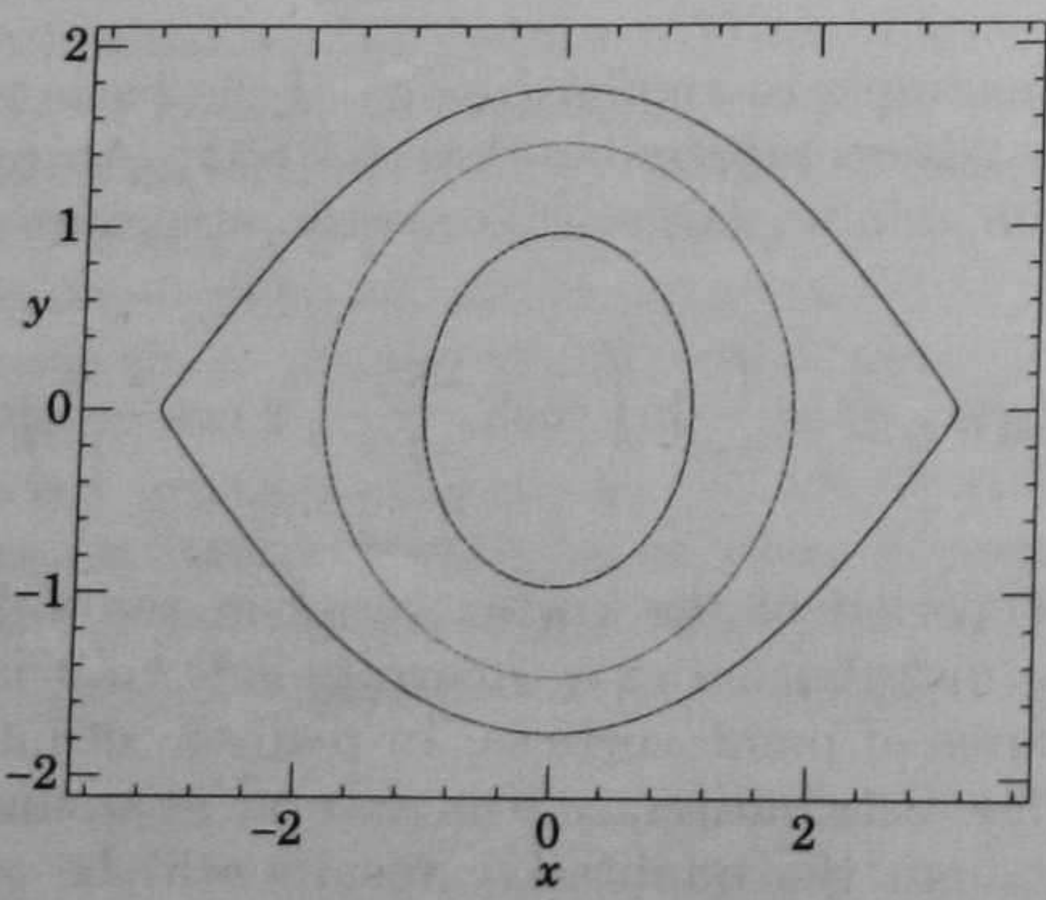

Fig. 3. – Orbits of system (2.10) for $\mu_0 = 0$ and $h = 1$.

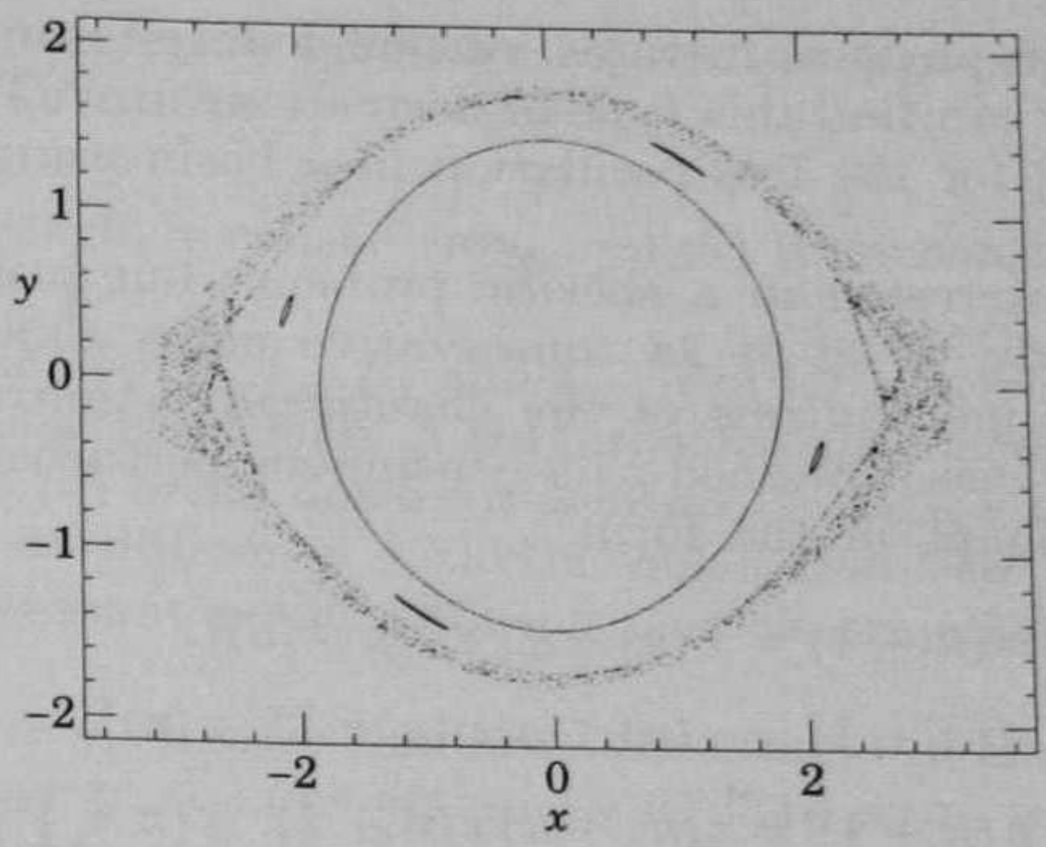

Fig. 4. – Iterations of the Poincaré map $\boldsymbol{x} = \boldsymbol{x}(n\pi)$, for three trajectories of system (2.10) with $\mu_0 = 0.01$, $h = 1.0$, $\omega = \Omega$. The trajectories started from $x_0 = 1.0$ and $y_0 = 1.5$ (the chaotic one), 1.4 (the four components one), 1.2 (the inner one).

a) chaotic behaviour for trajectories with initial conditions close to a separatrix;

b) regular motion if the initial conditions are far from the separatrices.

The area of the chaotic layer (the region of chaotic behaviour around the separatrix) increases with μ_0, and for large μ_0-values, it is practically impossible to distinguish between regular and chaotic regions.

In sect. **3** we shall show that such a scenario is not peculiar of a stream function whose time dependence is explicitly known, but it is also valid when the Eulerian equation passes from a steady solution to a time periodic solution, via a Hopf bifurcation.

We remark that for the case of time periodic velocity fields, *i.e.* $\boldsymbol{u}(\boldsymbol{x}, t + T) = \boldsymbol{u}(\boldsymbol{x}, t)$, where T is the period, the differential equation (1.1) describing the Lagrangian motion can be studied in terms of discrete dynamical systems. From standard theorems of the theory of differential equations, it is easy to see that one can determine the position $\boldsymbol{x}(t + T)$ in terms of $\boldsymbol{x}(t)$. Moreover, for periodic velocity field, the map $\boldsymbol{x}(t) \rightarrow \boldsymbol{x}(t + T)$ does not depend on t. The above arguments allows us to write (1.1) in the form

$$\boldsymbol{x}(n + 1) = \boldsymbol{F}[\boldsymbol{x}(n)], \tag{2.11}$$

where now the time is measured in units of the period T. If the incompressibility condition holds, the map (2.11) is conservative, *i.e.*

$$|\det \boldsymbol{A}[\boldsymbol{x}]| = 1, \quad \text{where} \quad A_{ij}[\boldsymbol{x}] = \frac{\partial F_i[\boldsymbol{x}]}{\partial x_j}.$$

An explicit deduction of the form of $\boldsymbol{F}$ for a general $2d$ or $3d$ flow is usually a very difficult task. However, in some simple cases, reasonable models,

containing the main physical features, can be deduced from the physics of the system. The reader can find this type of derivations in [CCTT87] for the Stokes flow, and in [LS89] for the free oscillation in a basin using the shallow-water approximation.

If one is not interested in a specific problem, but just in some «generic» properties, the study of $3d$ or $2d$ conservative maps allows us to determine many of the basic mechanisms of the chaotic advection.

A quite general case, obtained as a continuous perturbation of the identity map, is given by maps of the form

$$\begin{cases} x(n+1) = x(n) + f[y(n),\ z(n)], \\ y(n+1) = y(n) + g[x(n+1),\ z(n)], \\ z(n+1) = z(n) + h[x(n+1),\ y(n+1)]. \end{cases} \tag{2.12}$$

A straightforward calculation shows that regardless of the form of the three functions f, g and h, (2.12) is volume preserving. A simple nontrivial expression which captures the main features of $3d$ maps of the form (2.12) can be obtained by confining the three-dimensional dynamics on $3d$ torus and retaining only the lowest terms of the Fourier expansion of f, g and h. This procedure leads to

$$\begin{cases} x(n+1) = x(n) + A_1 \sin z(n) + C_2 \cos y(n), \\ y(n+1) = y(n) + B_1 \sin x(n+1) + A_2 \cos z(n), \\ z(n+1) = z(n) + C_1 \sin y(n+1) + B_2 \cos x(n+1). \end{cases} \tag{2.13}$$

Unfortunately, the knowledge of the properties of three-dimensional volume-preserving maps is not so rich as for symplectic maps [S83, S84]. However, one may try to use some ideas and methods developed for Hamiltonian systems [LL83].

For $B_i = C_i = 0$ the map (2.13) is trivially integrable and the motion of a fluid particle is restricted to the plane

$$z = z(0) = \text{const}. \tag{2.14}$$

For B_i and C_i of order $\varepsilon \ll 1$ (2.13) is a nonsymplectic perturbation of a two-dimensional integrable symplectic map. In this case, called in [FKP88] one-action three-dimensional Liouvillian map, a first-order perturbation theory shows that the invariant plane (2.14) survives, with small changes, in a KAM-like way. In other words, the invariant surface of the perturbed map can be written in the form

$$z = z(0) + \varepsilon \sum_{n,\,m} a_{nm} \exp[i(mx + ny)] + O(\varepsilon^2),$$

where $z(0)$ satisfies the condition of nonresonance. For example if $A_1 = A_2 \equiv A$, the first resonance is given by

$$mA \sin z(0) + nA \cos z(0) = 2\pi k, \qquad (m,\ n) \neq (\pm 1,\ 0),\ (0,\ \pm 1).$$

These results are in excellent agreement with numerical data.

Another case of interest is given by $A_1 = A_2 = B_1 = C_2 = 0$, where there are two conserved quantities:

$$x = x(0) = \text{const} \quad \text{and} \quad y = y(0) = \text{const}. \tag{2.15}$$

By analogy, the case of A_1, A_2, B_1 and C_2 of order $\varepsilon \ll 1$ is called two-action three-dimensional Liouvillian map. A perturbative approach shows that almost all invariant lines (2.15) break down for arbitrarily small ε and are replaced by invariant surfaces. At difference with the one-action case, they do intersect each other at the resonant point, allowing particle trajectories to diffuse over the entire space.

We therefore have a scenario similar to that found in Hamiltonian systems. Indeed, the behaviour of the one-action Liouvillian map, where the perturbed invariant curves divide the whole space into disjoint regions, is similar to two-dimensional Hamiltonian systems where the KAM tori separate the space into disconnected parts. On the other hand, the two-action Liouvillian maps, with trajectories diffusing over the whole space, is qualitatively similar to three-dimensional Hamiltonian systems where the KAM tori are not sufficient to divide the space into disjoint regions and Arnold diffusion [LL83] is believed to occur. Diffusion in two-action Liouvillian maps is, however, much faster than Arnold diffusion. In the latter case, the diffusion coefficient is exponentially small in ε, *i.e.* $O(\exp[-c/\varepsilon^{1/2}])$, while in the former is $O(\varepsilon^{\alpha})$ with $\alpha \simeq 2$ [FKP88].

Let us now turn our attention to two-dimensional systems. A quite general class of conservative systems is again given by maps of the form

$$\begin{cases} x(n+1) = x(n) + f[y(n)], \\ y(n+1) = y(n) + g[x(n+1)]. \end{cases} \tag{2.16}$$

A widely studied map of this family is the so-called standard map [C79]

$$\begin{cases} x(n+1) = x(n) + K \sin y(n), \\ y(n+1) = y(n) + x(n+1), \end{cases} \tag{2.17}$$

obtained by taking $f(y) = K \sin y$ and $g(x) = x$. The important parameter in (2.17) is K which measures the strength of the nonlinearity in the system. For small values of K the chaotic motion is limited to small regions and the mixing due to Lagrangian motion is rather poor. In fig. 5 is shown the spreading of a spot of particles at different times in such a situation. It is well evident the weak mixing in the x-direction. On the contrary for $K \gtrsim K_c \simeq 1$ the chaotic region covers practically the whole phase space. In this case the mixing becomes very efficient since the distance between initially close particles grows exponentially in time, see fig. 6.

The map (2.17) has no direct relation with any physical situation. Its importance relies on the fact that its behaviour is the typical behaviour of Lagrangian motion in time periodic velocity fields. We stress that the strong

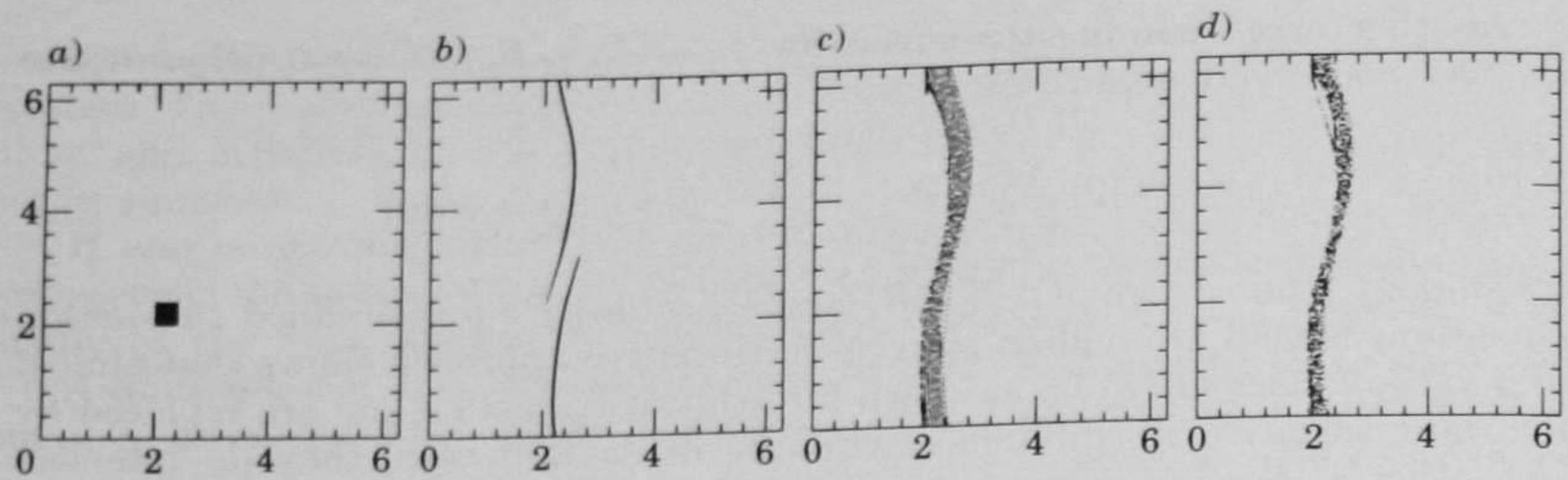

Fig. 5. – Evolution of 2500 test particles, initially located in the square $[2.0, 2.4] \times [2.0, 2.4]$, under the action of the standard map, eq. (2.17) with $K = 0.5$, shown at the times 0 (a)), 15 (b)), 100 (c)), 1000 (d)).

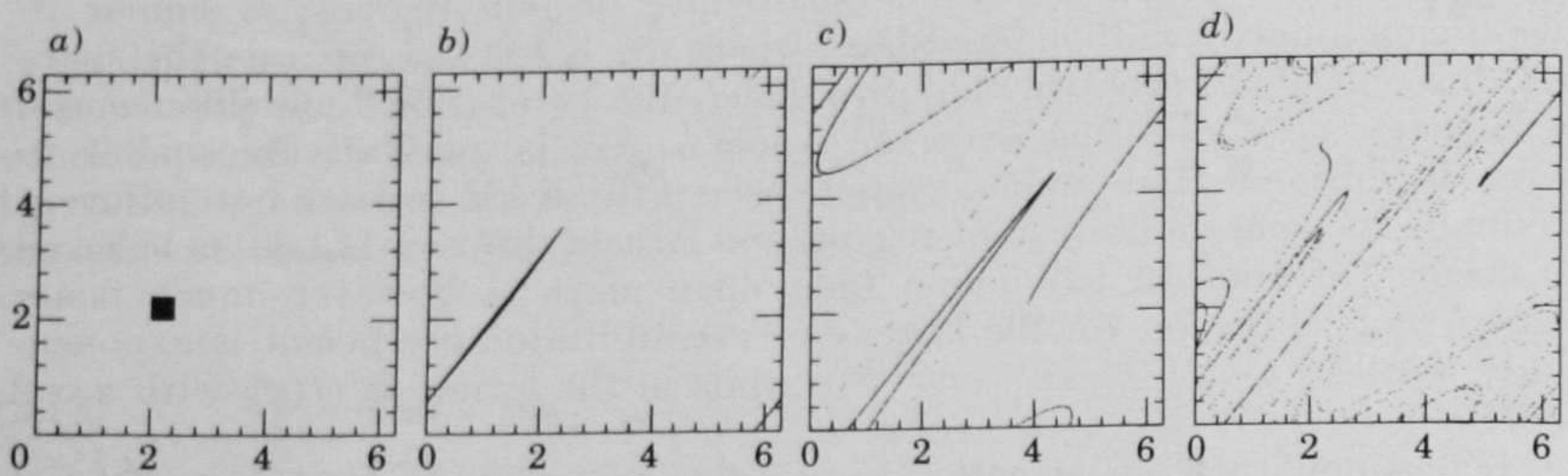

Fig. 6. – The same as fig. 5, but with $K = 3.4$, at the times 0 (a)), 2 (b)), 4 (c)), 6 (d)).

mixing properties for $K \gtrsim 1$ are only due to deterministic dynamics and the presence of small random terms do not change significantly this scenario. Figure 7 shows the spreading of a spot of points initially close when an additional random term is added to (2.17), *i.e.*

$$\begin{cases} x(n+1) = x(n) + K \sin y(n) + \varepsilon_1 \eta_1(n), \\ y(n+1) = y(n) + x(n+1) + \varepsilon_2 \eta_2(n), \end{cases} \tag{2.18}$$

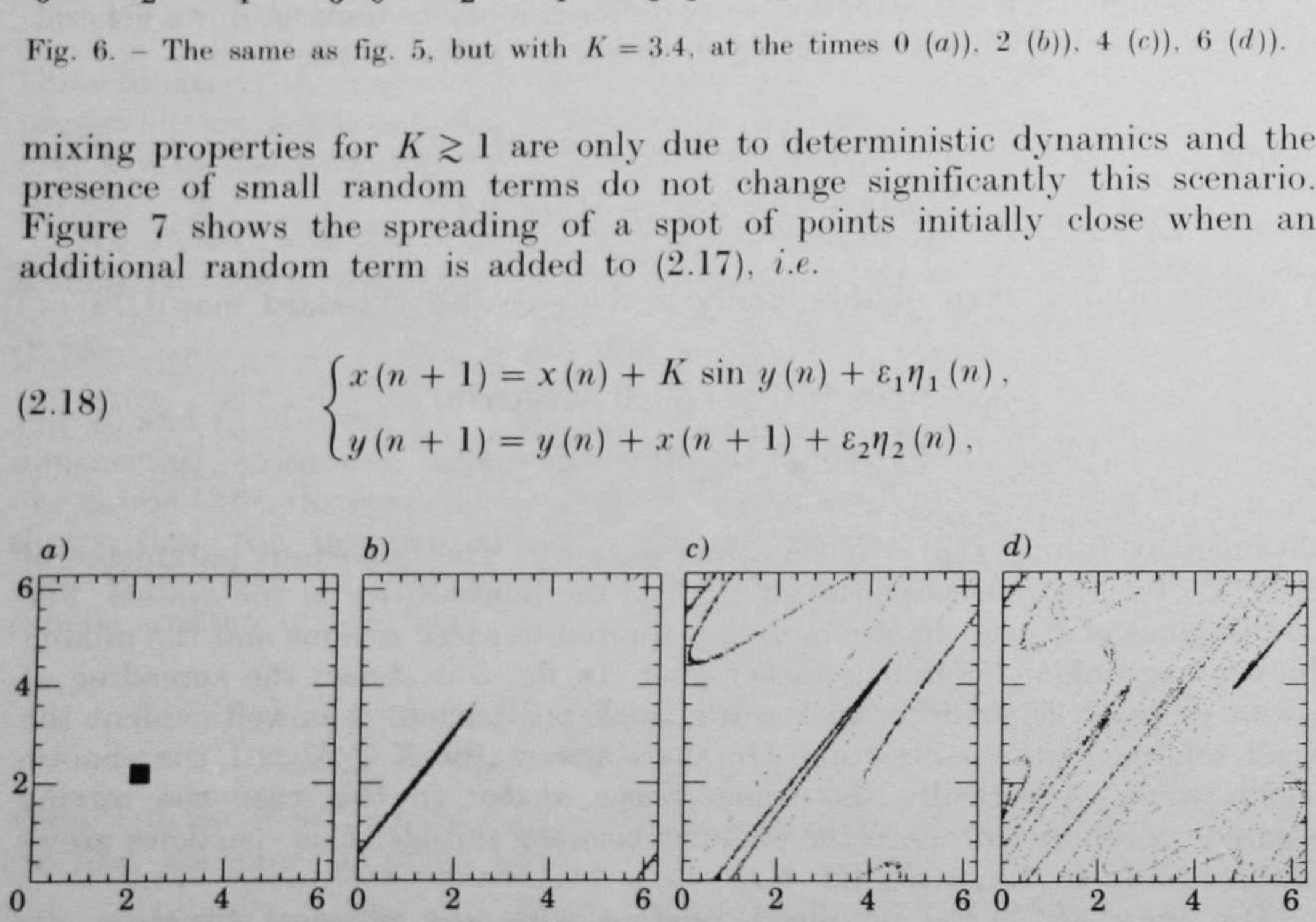

Fig. 7. – The same as fig. 6 with the addition of a noise: eq. (2.18) with $K = 3.4$, $\varepsilon_1 = 0.01$ and $\varepsilon_2 = 0.02$.

where $\eta_i(n)$ are Gaussian discrete processes of zero mean and correlation

$$\langle \eta_i(n)\eta_j(n')\rangle = \delta_{ij}\delta_{nn'}\,.$$

The comparison with fig. 6 enlights the weak role of randomness.

In some sense, a small random term in the evolution equations of test particles plays, in the Lagrangian description, a role analogous to that of molecular diffusion in the Eulerian approach. In sect. **5** we shall see that molecular diffusivity can have nontrivial effects on the diffusion properties also for steady two-dimensional velocity fields where (1.1) is integrable.

2˙**2**. *Stretching of material lines and surfaces.* – Many results obtained with phenomenological arguments in the theory of turbulence, or with the help of stochastic models [DM90, DM91], can be derived using ideas and methods borrowed from the theory of dynamical systems. This approach enlights the role of the Lagrangian chaos, and permits to extend the validity of these results to include situations without Eulerian turbulence.

The linearization of (1.1) around a solution $\boldsymbol{x}(t)$ leads to

$$\dot{z}_i = \sum_{j=1}^{d} \left.\frac{\partial u_i}{\partial x_j}\right|_{x(t)} z_i\,. \tag{2.19}$$

If we consider the vector $\delta\boldsymbol{x}$ joining two close fluid particles, (2.19) describes the evolution of a material line element $\delta\boldsymbol{x}$, if $|\delta\boldsymbol{x}|$ is small enough. Batchelor [B52] argued, on the basis of nonrigorous but very reasonable arguments, that for large times and small $|\delta\boldsymbol{x}(0)|$

$$|\delta\boldsymbol{x}(t)| \sim |\delta\boldsymbol{x}(0)|\exp[\alpha_1 t] \quad \text{with} \quad \alpha_1 > 0\,. \tag{2.20}$$

This result has been criticized by Cocke [C69, C71] who claimed that the argument of Batchelor, and hence the result (2.20), is not correct. Cocke's reasoning is also quoted by Monin and Yaglom [MY75] in one of the main textbook of fluid dynamics. The origin of this dispute is in an exchange of limits. If $\delta\boldsymbol{x}(0)$ is small enough α_1 is nothing but the effective Lyapunov exponent, whose most probable value is the first (maximum) Lyapunov exponent of (1.1), see subsect. **6**˙**3**. The Cocke's remark is based on his result that, under general assumptions, for large times in a turbulent fluid

$$|\delta\boldsymbol{x}(t)| \sim t^{1/2} \tag{2.21}$$

so that $t^{-1}\ln|\delta\boldsymbol{x}(t)|\to 0$ as $t\to\infty$, and therefore (2.20) cannot be valid. However (2.21) is derived for large times with fixed $|\delta\boldsymbol{x}(0)|$, *i.e.* for $t \gg (1/\alpha_1)\ln(L/|\delta\boldsymbol{x}(0)|)$, where L is a typical length. On the other hand, in (2.20) one takes the limit $|\delta\boldsymbol{x}(0)|\to 0$ first and then $t\to\infty$, and hence there is no contradiction between (2.20) and (2.21).

The problem of the growth of the area of a material surface element can be treated in a similar way. A small material surface is individuated by two nonparallel vectors $\delta\boldsymbol{x}_1(t)$ and $\delta\boldsymbol{x}_2(t)$ starting from the same point, and hence by two lengths $l_{1,2}(t) = |\delta\boldsymbol{x}_{1,2}(t)|$ and the angle between the two vectors. If l_i

is small enough $\delta \boldsymbol{x}_i(t)$ obeys (2.19) and the area of the material surface is given by

$$\delta \mathscr{S}(t) = |\delta \boldsymbol{x}_1(t) \times \delta \boldsymbol{x}_2(t)| \sim \delta \mathscr{S}(0) \exp[\alpha_2 t], \tag{2.22}$$

where « × » denotes the external (cross) product. By denoting with $\lambda_1 \geq \lambda_2 \geq \lambda_3$ the characteristic Lyapunov exponents of (1.1) we have that the most probable value of α_2 is $\lambda_1 + \lambda_2$, see subsect. **6**·3.

A general theorem states that for $3d$ steady velocity fields at least one of the characteristic Lyapunov exponenets should be zero. Moreover, the incompressibility condition requires that $\lambda_1 + \lambda_2 + \lambda_3 = 0$ so that in a chaotic system one should have $\lambda_2 = 0$, since $\lambda_1 > 0$. In this case, the typical growth of a surface element coincides with that of a line element.

Feingold *et al.* [FKP88] found $\lambda_2 = 0$ also for a generic three-dimensional time-periodic velocity field described by a conservative three-dimensional map. On this basis they argued that this result should hold in general as a consequence of the conservative nature of the Lagrangian motion in incompressible fluids.

It is not difficult to extend (2.20) and (2.22) to *finite* material lines and surfaces.

The problem of the probability distribution of $l(t)$ and $\delta \mathscr{S}(t)$ can also be analysed in terms of dynamical systems. Since by definition $l(t) = |\delta \boldsymbol{x}(t)|$ and $\delta \mathscr{S}(t) = |\delta \boldsymbol{x}_1(t) \times \delta \boldsymbol{x}_2(t)|$, the statistics of the length of a material line element and of the area of a material surface element are given by the statistics of the response functions

$$R^{(1)}(t) = \frac{|\boldsymbol{z}^{(1)}(t)|}{|\boldsymbol{z}^{(1)}(0)|} \quad \text{and} \quad R^{(2)}(t) = \frac{|\boldsymbol{z}^{(1)}(t) \times \boldsymbol{z}^{(2)}(t)|}{|\boldsymbol{z}^{(1)}(0) \times \boldsymbol{z}^{(2)}(0)|},$$

respectively, where $\boldsymbol{z}^{(i)}(t)$ obeys (2.19). The interested reader is referred to subsect. **6**·3 for technical details.

The probability distribution $\mathscr{P}[l(t)]$ of $l(t)$ is not universal and its details strongly depend on the features of the dynamical system (1.1). Nevertheless for large times, $\mathscr{P}[l(t)]$ is close to a log-normal distribution (see subsect. **6**·3)

$$\mathscr{P}[l(t)] \simeq \frac{1}{l(t)\sqrt{2\pi\mu t}} \exp\left[-\left(\ln\left[\frac{l(t)}{l(0)}\right] - \lambda_1 t \right)^2 \Big/ 2\mu t \right], \tag{2.23}$$

where

$$\mu = \lim_{\tau \to \infty} \frac{1}{\tau} \overline{(\ln z(\tau) - \lambda_1 \tau)^2}.$$

A similar result can be obtained for $\mathscr{P}[\delta \mathscr{S}(t)]$.

The above results, usually derived in the context of turbulence and/or probabilistic models [DM90, DM91], are only related to the presence of Lagrangian chaos and not to Eulerian turbulence. In fact, they can be obtained as simple application of rather general methods of the theory of dynamical systems.

3. – Eulerian behaviour and Lagrangian chaos.

The relation between Lagrangian and Eulerian chaos is a very complicated issue, also in extreme cases, *e.g.*, fully developed turbulence — see ref. [C62, L62]. In this section we shall discuss two different problems: the onset of Lagrangian chaos in relation with the features of the velocity field, and the effects of the presence of Eulerian chaos on the motion of fluid particles. In principle, the evolution of the velocity field $\boldsymbol{u}$ is described by partial derivative equations, such as the Navier-Stokes equations. However, a good approximation can be obtained by using a Galerkin approach, and reducing the Eulerian problem to a system of F ordinary differential equations (see subsect. **6**·5). The motion of a fluid particle is then described by the $(d + F)$-dimensional dynamical system

$$\frac{\mathrm{d}\boldsymbol{Q}}{\mathrm{d}t} = \boldsymbol{f}(\boldsymbol{Q}, t) \quad \text{with} \quad \boldsymbol{Q}, \boldsymbol{f} \in \boldsymbol{R}^F , \tag{3.1a}$$

$$\frac{\mathrm{d}\boldsymbol{x}}{\mathrm{d}t} = \boldsymbol{u}(\boldsymbol{x}, \boldsymbol{Q}, t) \quad \text{with} \quad \boldsymbol{x}, \boldsymbol{u} \in \boldsymbol{R}^d , \tag{3.1b}$$

where d is the space dimensionality and $\boldsymbol{Q} = (Q_1, \ldots Q_F)$ are the F variables, usually normal modes, which describe the evolution of the velocity field $\boldsymbol{u}$. Note that the Eulerian equations (3.1a) do not depend on the Lagrangian part (3.1b) and can be solved independently.

In order to characterize the degree of chaos, we can introduce three different Lyapunov exponents:

a) λ_{E} for the Eularian part (3.1a);

b) λ_{L} for the Lagrangian part (3.1b), where the evolution of the velocity field is assumed to be known;

c) λ_{T} for the total system of the $d + F$ equations.

These Lyapunov exponents are defined as

$$\lambda_{\mathrm{E,L,T}} = \lim_{t \to \infty} \frac{1}{t} \ln \frac{|\boldsymbol{z}(t)^{\mathrm{E,L,T}}|}{|\boldsymbol{z}(0)^{\mathrm{E,L,T}}|} , \tag{3.2}$$

where the evolution of the three tangent vectors $\boldsymbol{z}$ are given by the linearized stability equations for the Eulerian part, for the Lagrangian part and for the total system, respectively:

$$\frac{\mathrm{d}z_i^{(\mathrm{E})}}{\mathrm{d}t} = \sum_{j=1}^{F} \left.\frac{\partial f_i}{\partial Q_j}\right|_{Q(t)} z_j^{(\mathrm{E})} , \qquad \boldsymbol{z}^{(\mathrm{E})} \in \boldsymbol{R}^F , \tag{3.3a}$$

$$\frac{\mathrm{d}z_i^{(\mathrm{L})}}{\mathrm{d}t} = \sum_{j=1}^{d} \left.\frac{\partial u_i}{\partial x_j}\right|_{x(t)} z_j^{(\mathrm{L})} , \qquad \boldsymbol{z}^{(\mathrm{L})} \in \boldsymbol{R}^d , \tag{3.3b}$$

$$\frac{\mathrm{d}z_i^{(\mathrm{T})}}{\mathrm{d}t} = \sum_{j=1}^{d+F} \left.\frac{\partial G_i}{\partial y_j}\right|_{y(t)} z_j^{(\mathrm{T})} , \qquad \boldsymbol{z}^{(\mathrm{T})} \in \boldsymbol{R}^{F+d} , \tag{3.3c}$$

where $\boldsymbol{y} = (Q_1, \ldots, Q_F, x_1, \ldots, x_d)$ and $\boldsymbol{G} = (f_1, \ldots, f_F, u_1, \ldots, u_d)$. The meaning of these Lyapunov exponents is rather evident:

a) λ_E is the mean exponential rate of the increasing of the uncertainty in the knowledge of the velocity field;

b) λ_L estimates the rate at which the distance $\delta\boldsymbol{x}(t)$ between two fluid particles initially close increases with time, when the velocity field is given, *i.e.* a particle pair in the same Eulerian realization: $\delta\boldsymbol{x}(t) \sim \exp[\lambda_L t]$;

c) λ_T is the rate of growth of the distance between initially close particle pairs, when the velocity field is not known with infinite precision.

There is no general relation between λ_E and λ_L. One could expect that in the presence of a chaotic velocity field the particle motion has to be chaotic. However, the inequality $\lambda_L \geq \lambda_E$ — even if generic — does not hold in some systems like the Lorenz model (see subsect. **3**·2).

On the other hand, from (3.3*c*), one sees that

$$\lambda_T = \max(\lambda_E, \lambda_L). \tag{3.4}$$

This follows by noting that the stability matrix $(\boldsymbol{A}^T)_{ij} = \partial G_i/\partial y_j$ for the Eulerian plus Lagrangian system (3.3*c*) can be written as

$$\boldsymbol{A}^{(T)} = \begin{pmatrix} \boldsymbol{A}^{(E)} & \boldsymbol{0} \\ \boldsymbol{U} & \boldsymbol{A}^{(L)} \end{pmatrix}, \tag{3.5}$$

where $\boldsymbol{0}$ is the $F \times d$ zero matrix, and

$$A^{(E)}_{kl} = \frac{\partial f_k}{\partial Q_l}, \quad \text{of size} \quad F \times F,$$

$$A^{(L)}_{kn} = \frac{\partial u_k}{\partial x_n}, \quad \text{of size} \quad d \times d,$$

$$U_{ml} = \frac{\partial u_m}{\partial Q_l}, \quad \text{of size} \quad d \times F.$$

A direct computation shows that the matrix which gives the evolution in the tangent space is

$$\boldsymbol{M}^{(T)}[\boldsymbol{Q}(0), \boldsymbol{x}(0), t] = \exp\left[\int_0^t d\tau \boldsymbol{A}^{(T)}[\boldsymbol{Q}(\tau), \boldsymbol{x}(\tau)]\right]$$

and has a block tridiagonal structure. The eigenvalues are therefore the eigenvalues of the two diagonal blocks,

$$\boldsymbol{M}^{(E)}[\boldsymbol{Q}(0), t] = \exp\left[\int_0^t d\tau \boldsymbol{A}^{(E)}[\boldsymbol{Q}(\tau)]\right],$$

and

$$\boldsymbol{M}^{(L)}[\boldsymbol{Q}(0), \boldsymbol{x}(0), t] = \exp\left[\int_0^t d\tau \boldsymbol{A}^{(L)}[\boldsymbol{Q}(\tau), \boldsymbol{x}(\tau)]\right].$$

As a consequence the spectrum of the Lyapunov exponents of the total system is just the sum of the spectra of the Eulerian and Lagrangian part.

3·1. *Onset of Lagrangian chaos in two-dimensional fluids, a general mechanism: the Hopf bifurcation.* – We have discussed as in three dimensions Lagrangian chaos is present even in stationary velocity fields. In this case, it seems rather hopeless to search for a generic mechanism for the onset of an irregular motion of fluid particles in terms of the Eulerian behaviour.

This is no more true in two dimensions for incompressible fluids where the continuity equation $\nabla \cdot \boldsymbol{u} = 0$ is automatically satisfied by writing the velocity components as derivatives of a stream function $\psi(x, y)$. The Lagrangian equations of motion become

$$\frac{\mathrm{d}x}{\mathrm{d}t} = u_x = \frac{\partial \psi}{\partial y}, \qquad \frac{\mathrm{d}y}{\mathrm{d}t} = u_y = -\frac{\partial \psi}{\partial x}, \tag{3.6}$$

where we use the notation $x \equiv x_1$, $y \equiv x_2$ for the space-coordinates of the fluid particle. The stream function is formally the Hamiltonian of a one-dimensional system whose generalized coordinate and momentum are x and y. This allows us to connect the Lagrangian chaos with the behaviour of the velocity field. In fact, it is well known that one-dimensional systems are integrable if energy is conserved. A chaotic behaviour is therefore possible only for time-dependent Hamiltonian when there are no integrals of motion. There exists a wide literature on quasi-integrable systems. In particular, the effects of time-dependent perturbations on autonomous one-dimensional Hamiltonian systems are well understood.

For our purposes, we shall consider the Navier-Stokes equations (2.5) at low Reynolds numbers, in two dimensions and with periodic boundary conditions. A convenient way to study the Lagrangian behaviour is by means of truncated models of these equations. These are obtained by expanding the stream function ψ in Fourier series and taking into account only the first F terms [BF79, L87].

$$\psi = -i \sum_{j=1}^{F} k_j^{-1} Q_{k_j} \exp[ik_j x] + \text{c.c.}, \tag{3.7}$$

where c.c. indicates the complex conjugate term and $\boldsymbol{Q} = (Q_1, \ldots, Q_F)$ are the F variables (normal modes) which describe the Eulerian field evolution. Inserting (3.7) into the Navies-Stokes equations and, by an appropriate time rescaling, we obtain the system of F ordinary differential equations

$$\frac{\mathrm{d}Q_j}{\mathrm{d}t} = -k_j^2 Q_j + \sum_{l,m} A_{jlm} Q_l Q_m + f_j \tag{3.8}$$

with $j = 1, \ldots, F$ and f_j represents the effect of the external forcing on the j mode. For an explicit form of the coefficients A_{jlm} see subsect. 6·5.

Franceschini and coworkers have studied this truncated model with $F = 5$ and $F = 7$ [BF79, L87]. Here we shall discuss the Lagrangian behaviour of a fluid particle at varying Reynolds number, Re, defined in (3.8) through $\boldsymbol{f}$. By using the parameters introduced in [BF79] it turns out $f_j = \mathrm{Re}\,\delta_{j,3}$. Let us

consider the case of $F = 5$ modes. For $\mathrm{Re} < \mathrm{Re}_1 = 22.8537...$, there are four stable stationary solutions, say $\hat{\boldsymbol{Q}}$, so that $\lambda_E < 0$. At $\mathrm{Re} = \mathrm{Re}_1$, these solutions become unstable, via a Hopf bifurcation [MM75], and four stable periodic orbits appear, implying $\lambda_E = 0$. For $\mathrm{Re}_1 < \mathrm{Re} < \mathrm{Re}_2 = 28.41...$, one thus finds the stable limit cycles:

$$\boldsymbol{Q}(t) = \hat{\boldsymbol{Q}} + (\mathrm{Re} - \mathrm{Re}_1)^{1/2} \delta\boldsymbol{Q}(t) + O(\mathrm{Re} - \mathrm{Re}_1), \tag{3.9}$$

where $\delta\boldsymbol{Q}(t)$ is periodic with period

$$T(\mathrm{Re}) = T_0 + O(\mathrm{Re} - \mathrm{Re}_1), \qquad T_0 = 0.73277... \tag{3.10}$$

At $\mathrm{Re} = \mathrm{Re}_2$, these limit cycles lose stability and there is a period-doubling cascade toward Eulerian chaos.

For $\mathrm{Re} < \mathrm{Re}_1$, the stream function is asymptotically stationary, $\psi(\boldsymbol{x}, t) \to \psi(\boldsymbol{x})$, and the corresponding one-dimensional Hamiltonian is time independent. The Bendixson-Poincaré theorem [A72] and the continuity equation $\nabla \cdot \boldsymbol{u} = 0$ imply that the solutions of the Lagrangian equation (3.1*b*) are regular: fixed points and periodic or unbounded orbits. In fig. 8 we report the structure of the separatrices, *i.e.* orbits of infinite period, at $\mathrm{Re} = \mathrm{Re}_1 - 0.05$. One can observe the presence of hyperbolic fixed points and of two kinds of separatrices: the isolated «eights», labelled by A, and the connected periodic separatrices, labelled by B. For $\mathrm{Re} = \mathrm{Re}_1 + \varepsilon$ the stream function becomes time dependent:

$$\psi(\boldsymbol{x}, t) = \hat{\psi}(\boldsymbol{x}) + \sqrt{\varepsilon}\, \delta\psi(\boldsymbol{x}, t) + O(\varepsilon), \tag{3.11}$$

where $\hat{\psi}(\boldsymbol{x})$ is given by $\hat{\boldsymbol{Q}}$ and $\delta\psi$ is periodic in $\boldsymbol{x}$ and in t with period T. The region of phase space, here the real two-dimensional space, adjacent to a separatrix is very sensitive to perturbations, even of very weak intensity. Indeed, generically in one-dimensional Hamiltonian systems, a periodic perturbation

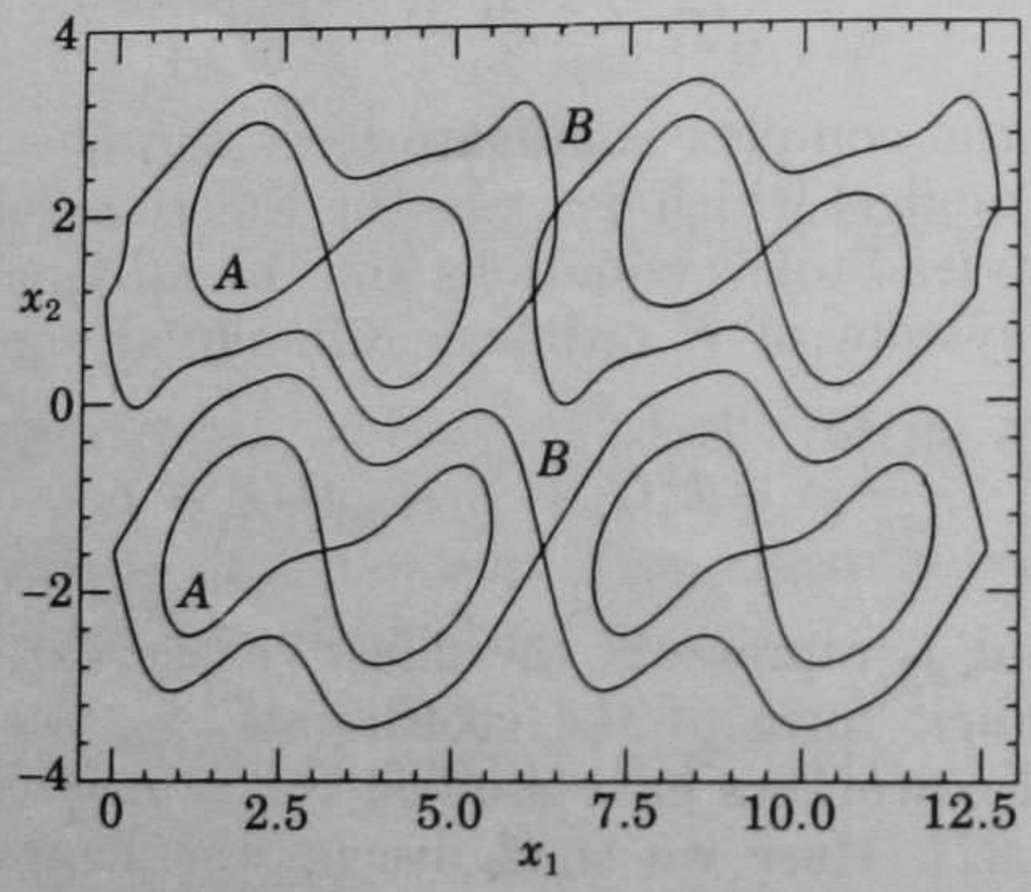

Fig. 8. – Structure of the separatrices of eq. (3.6), with ψ given by eqs. (3.7) and (3.8), in the 5-modes truncation case (see subsect. **6**·5) with $\mathrm{Re} = \mathrm{Re}_1 - 0.05$.

gives origin to stochastic layers around the separatrices where the motion is chaotic, as a consequence of unfolding and crossing of the stable and unstable manifolds in domains centred at the hyperbolic fixed points (see, for instance, [LL83]). A method due to Melnikov [M63] allows us to prove the existence and to estimate the size of a stochastic layer for Hamiltonian systems close to integrability, if the unperturbed solution on the separatrix is known. However, here for the truncated models of Navier-Stokes equations, we are not able to use this method, since the structure of the Hamiltonian, *i.e.* of the stream function ψ, is rather complicated. One can only provide a numerical evidence for the existence of the chaotic regions, by computing the maximum Lyapunov exponent. We show in fig. 9 a picture of the chaotic and regular motion for small ε by means of the Poincaré map

$$\boldsymbol{x}(nT) \rightarrow \boldsymbol{x}(nT + T)\,. \tag{3.12}$$

The period $T(\varepsilon)$ is computed numerically. The size of the stochastic layers rapidly increases with ε. At $\varepsilon \approx 0.7$ they overlap and it is practically impossible to distinguish between regular and chaotic zones. Four different behaviours are observed at increasing ε:

a) a chaotic motion bounded in the stochastic layers originated by the separatrices of type A;

b) an unbounded chaotic motion in the stochastic layers originated by the separatrices of type B;

c) an unbounded regular motion in the regions separated by stochastic layers of type B;

d) a bounded regular motion in the regions inside stochastic layers of type B but far enough from the stochastic layers of type A.

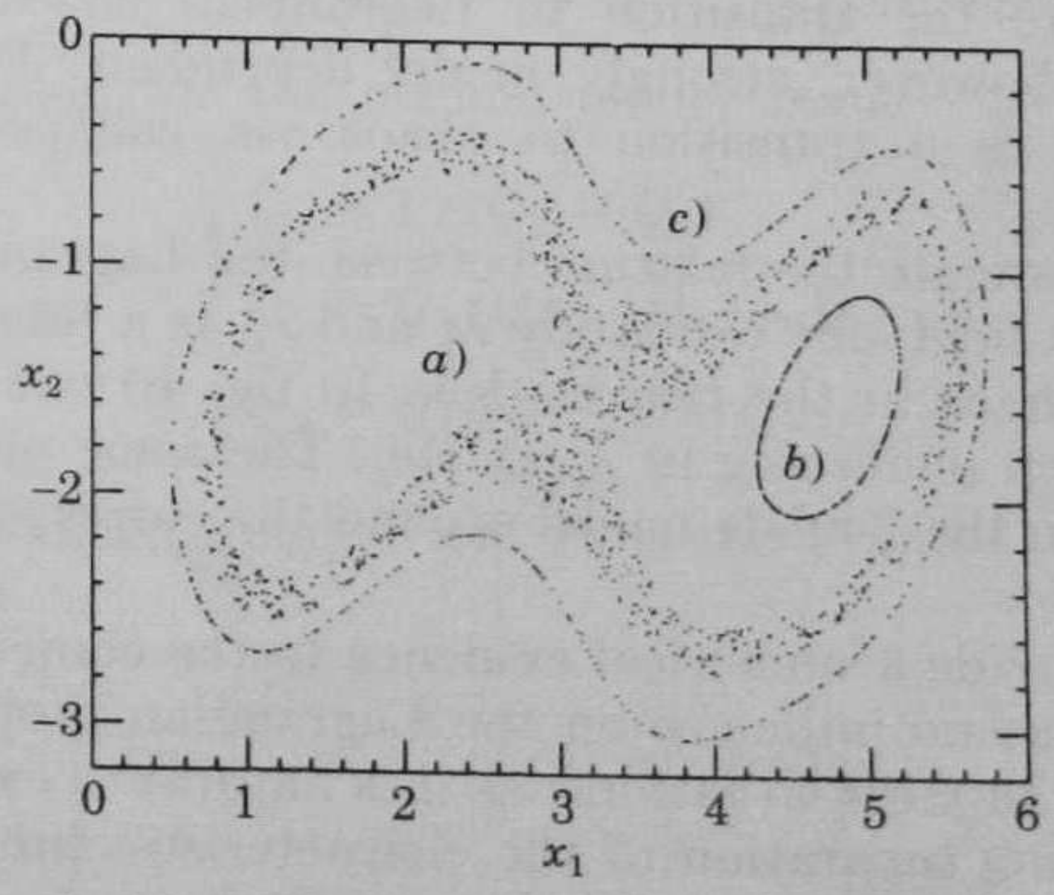

Fig. 9. – Poincaré map for three trajectories of system (3.6) in the 5-modes model with $\mathrm{Re} = \mathrm{Re}_1 + 0.05$. The initial conditions are selected close to a separatrix, case *a*) ($x_1(0) = 3.2$, $x_2(0) = -1.6$), or far from the separatrices, cases *b*) ($x_1(0) = 4.3$, $x_2(0) = -2.0$) and *c*) ($x_1(0) = 4.267$, $x_2(0) = -3.009$).

At $\varepsilon > \varepsilon_c \simeq 0.7$ the chaotic regions overlap and there is always a diffusive motion. We shall return on this point in sect. **5**.

This scenario for the onset of Lagrangian turbulence in two-dimensional fluids is generic and does not depend on the particular truncated model. In fact, it is only related to the appearance of stochastic layers under the effects of small time-dependent perturbations in one-dimensional integrable Hamiltonian systems. As a consequence of general features of one-dimensional Hamiltonian systems we expect that a stationary stream function becomes time periodic through a Hopf bifurcation. This is the case for all known truncated models of Navier-Stokes equations. By contrast the diffusion behaviours are strongly related to the detailed structure of the velocity fields, for more details see sect. **5**.

This scenario of transition to Lagrangian chaos cannot be applied to three-dimensional fluids, where stationary velocity fields may support Lagrangian chaos. We do not expect that the presence of a Hopf bifurcation in the solution of the Eulerian equation plays any role in three dimensions, except perhaps quite particular situations [FKP88].

3·2. *Eulerian chaos and fluid particle motion.* – It is rather evident that there is no simple relation between Eulerian and Lagrangian behaviours. In the following, we shall discuss two important points:

i) what are the effects on the Lagrangian chaos of the transition to Eulerian chaos, *i.e.* from $\lambda_E = 0$ to $\lambda_E > 0$;

ii) whether a chaotic velocity field ($\lambda_E > 0$) should imply a stochastic motion of fluid particles.

The first point can be again studied with the truncated models of two-dimensional Navier-Stokes equations. For the previous model with $F = 5$ modes, the limit cycles bifurcate to new double period orbits at $\mathrm{Re} = 28.41$. Then, there is a period-doubling transition to chaos and a strange attractor in the $\boldsymbol{Q}$ space appears at $\mathrm{Re}_c \approx 28.73$, where λ_E becomes positive.

Note that unlike the transition to Lagrangian chaos, the transition to Eulerian chaos is, however, strongly model dependent. For example, in the $F = 7$ model there is a transition to chaos via collapsing of periodic orbits [L87].

In order to investigate the relation between the Lagrangian behaviour and that of the Eulerian field, one can study λ_E and λ_L as a function of Re near the onset of Eulerian chaos in the two models. In fig. 10 one sees that λ_L is not affected by the sharp increasing of λ_E at Re_c. The same qualitative behaviour has been observed in the 7-mode model around the corresponding critical value $\mathrm{Re}_c \approx 555$.

These results provide a numerical evidence to the conjecture that the onset of Eulerian chaos has no influence on the Lagrangian properties. This conjecture should be valid in most situations, as it is natural to expect that in generic cases there is a strong separation of the characteristic times for Eulerian and Lagrangian behaviours.

The second point – the conjecture that a chaotic velocity field implies a chaotic motion of particles – could also look very natural. Indeed, it appears to hold in many systems, and in particular in the truncated models. Neverthe-

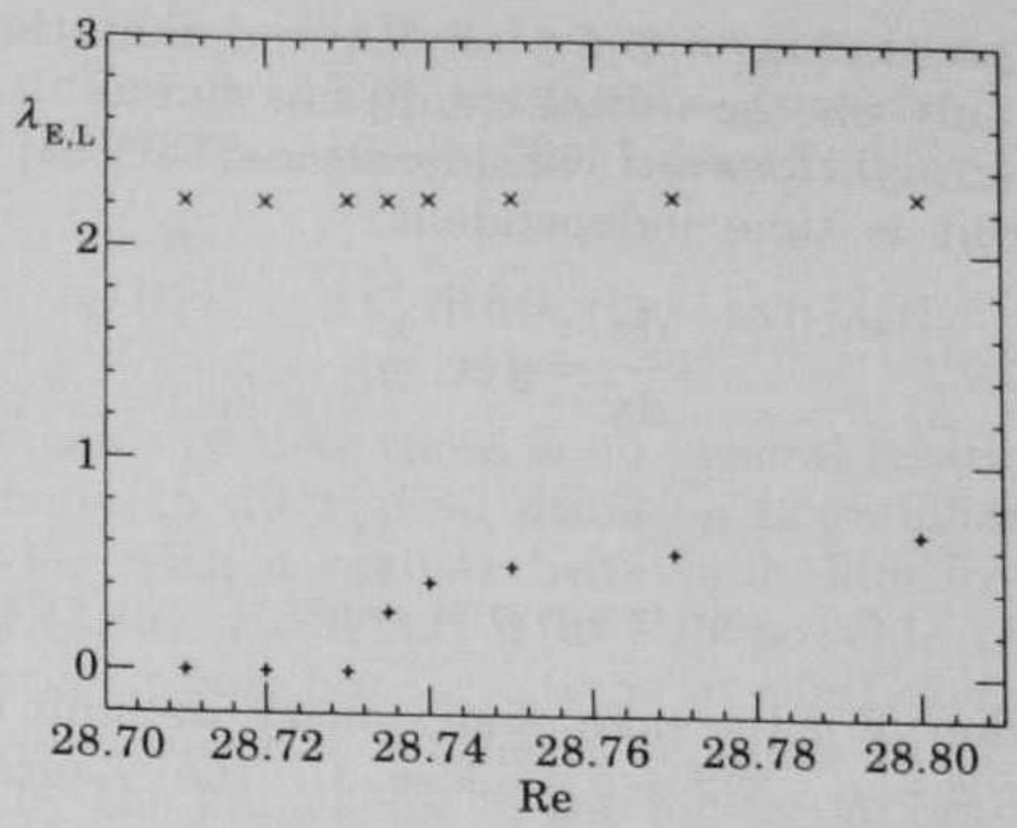

Fig. 10. – The Lyapunov exponenets λ_E (+) and λ_L (×) (eqs. (3.2), (3.3)) as functions of Re, around Re_c, for the 5-mode model.

less, one can find a class of systems where this is not true, *i.e.* the system (3.1) may exhibit a chaotic behaviour with $\lambda_E > 0$, while $\lambda_L = 0$.

This is the case, for example, of one of the most famous chaotic systems, the Lorenz model [L63]. Indeed, it exhibits the surprising feature of Eulerian chaos without Lagrangian chaos. The Lorenz model is obtained with some rude simplifications from the equations for the convection of the temperature in a slide of fluid, say (x, y)-plane, with a gravitational field and a temperature gradient directed along y. Here there are $F = 3$ degrees of freedom and, hence, three variables Q_1, Q_2 and Q_3 related to the stream function and to the displacement of temperature σT from the linear behaviour (in y) in the absence of convection:

$$\begin{cases} \psi = Q_1 \sin x \sin y\,, \\ \delta T = \sqrt{2}\, Q_2 \cos x \sin y - Q_3 \sin 2y\,. \end{cases} \tag{3.13}$$

The Eulerian equation for the normal modes reads

$$\begin{cases} \dot{Q}_1 = \mathrm{Pr}\,(Q_2 - Q_1)\,, \\ \dot{Q}_2 = Q_1\,(\mathrm{Ra} - Q_3) - Q_2\,, \\ \dot{Q}_3 = Q_1 Q_2 - (8/3)\, Q_3\,. \end{cases} \tag{3.14}$$

where Ra is the Rayleigh number and Pr is the Prandtl number. The Lagrangian equations are

$$\begin{cases} \dot{x} = \dfrac{\partial \psi}{\partial y} = \sqrt{2}\, Q_1\,(t) \sin x \cos y\,, \\ \dot{y} = -\dfrac{\partial \psi}{\partial x} = -\sqrt{2} Q_1\,(t) \cos x \sin y\,, \end{cases} \tag{3.15}$$

where $x,\ y \in [0,\ \pi]$ and t are rescaled dimensionless variables.

It is possible to show that $\lambda_L = 0$ for all Ra and that the orbits are always closed and depend only on the initial conditions but not on Ra. This can be explained by some straightforward considerations [FPV88] by noting that the equation for the orbit is time independent:

$$\frac{dx}{dy} = g(x, y)$$

and that

$$\sin x \sin y = \text{const}$$

is an integral of motion. For the sake of simplicity we limit the discussion to an initial condition $(\pi/2 + q_1, \pi/2 + q_2)$ close to the Lagrangian fixed point $(\pi/2, \pi/2)$. One thus has

$$\begin{cases} \frac{dq_1}{dt} = -\sqrt{2}\, Q_1(t)\, q_2 , \\ \frac{dq_2}{dt} = \sqrt{2}\, Q_1(t)\, q_1 . \end{cases} \tag{3.16}$$

By integrating (3.16) in polar coordinates, one obtains

$$r(t) = \text{const} \quad \text{and} \quad \phi(t) = \phi(0) + \sqrt{2}\int_0^t d\tau Q_1(\tau) . \tag{3.17}$$

This result implies that the particles move on a circle of radius r with angular velocity $\sqrt{2}\, Q_1(t)$. The motion can be chaotic for appropriate values of the control parameter Ra since $Q_1(t)$ itself can be chaotic. The Lagrangian Lyapunov exponent is $\lambda_L = 0$ for all Ra since both δr and $\delta\phi$ are constant in time, and hence two particles initially close remain close in the same realization of the velocity field. In spite of this, the Lagrangian motion of the particles looks chaotic when $\lambda_E > 0$ (see fig. 11), if the velocity field is not known with infinite

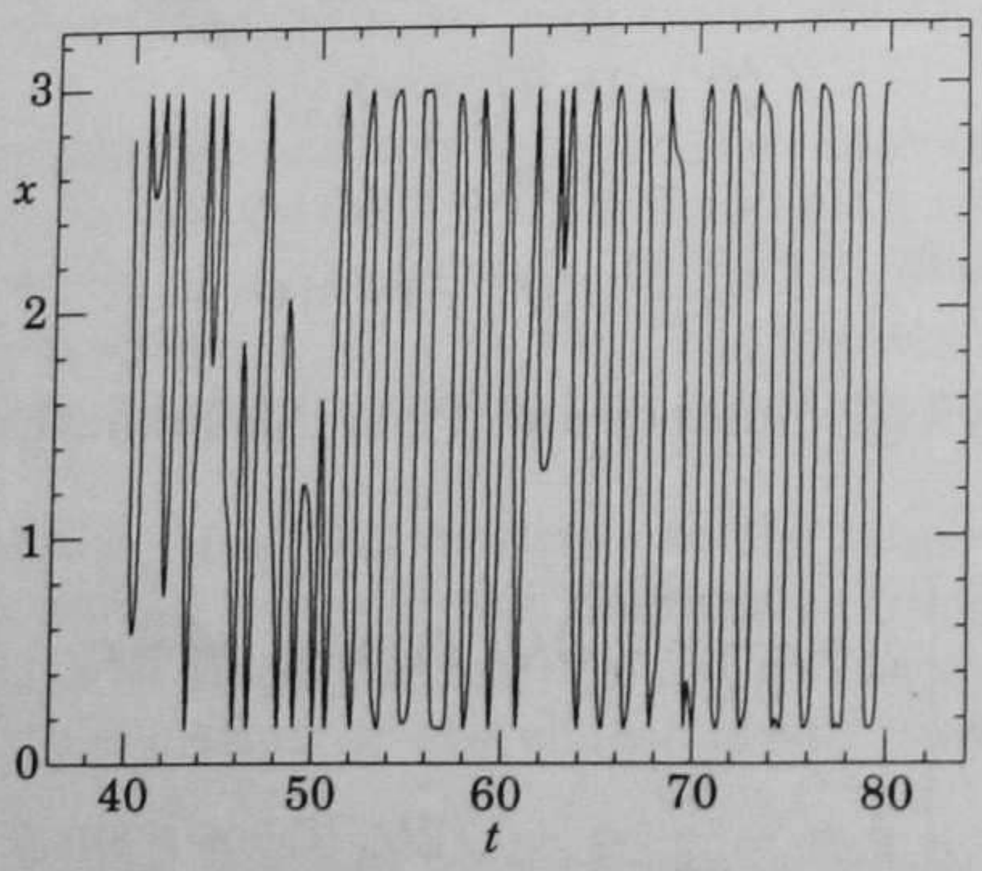

Fig. 11. – The Lagrangian coordinate $x(t)$ for the Lorenz model with Ra = 26.24 and Pr = 10 (the Eulerian part, eq. (3.14), is chaotic).

precision, since in this case the total Lyapunov exponent $\lambda_T = \lambda_E$, see (3.4). Indeed, the phase difference $\delta\phi(t)$ between a particle in the velocity field described by $\boldsymbol{Q}$ and one in the velocity field described by $\boldsymbol{Q} + \delta\boldsymbol{Q}$ increases as

$$\delta\phi(t) = \sqrt{2}\int_0^t \mathrm{d}\tau \delta Q_1(\tau) \sim \exp[\lambda_E t]. \tag{3.18}$$

In conclusion we can say that there is no general relation between Lagrangian and Eulerian chaos. In the typical situation Lagrangian chaos may appear also for velocity fields with a regular behaviour, like in the case of the $2d$ incompressible fluid (3.13). However, it is also possible to have the opposite situation, with Eulerian chaos but $\lambda_L = 0$, as in the Lorenz model. We finally stress that, in any case, one is not able to separate the Lagrangian from the Eulerian properties by the knowledge of the motion of only one trajectory, *e.g.* a buoy in the oceanic currents [OKPB86]. Indeed, using the standard data treatment methods [GP83], from $\boldsymbol{x}(t)$ one extracts the total Lyapunov exponent λ_T and not λ_L or λ_E. Nevertheless, one can detect λ_L by looking at the time behaviour of a scalar field in two close points $\boldsymbol{x}$ and $\boldsymbol{x}'$. From (1.6) one has

$$\Theta(\boldsymbol{x}, t) - \Theta(\boldsymbol{x}', t) \simeq \sum_{i=1}^{d} \frac{\partial\Theta_0}{\partial(\boldsymbol{T}^{-t}\boldsymbol{x})_i}(\boldsymbol{T}^{-t}\boldsymbol{x} - \boldsymbol{T}^{-t}\boldsymbol{x}')_i \sim \exp[\lambda_L t].$$

Note once more that the knowledge of the scalar field in one point $\boldsymbol{x}$ in principle is not sufficient to decide whether the Lagrangian chaos is present or not. One needs at least a two-point statistics. For example in the Lorenz model one observes a very irregular behaviour of $\Theta(\boldsymbol{x}, t)$, while $\Theta(\boldsymbol{x}, t) - \Theta(\boldsymbol{x}', t)$ increases only polynomially with t.

4. – Statistics of passive fields.

A chapter of remarkable interest in the physics of fluids concerns the study of the dispersive properties of flows on the distribution of some local property of fluids. In most cases these distributions refer either to scalar quantities, Θ, whose total amount associated with a material volume of fluid is conserved, or to vectorial quantities, $\boldsymbol{F}$, whose flux through an open material surface of fluid is conserved. The dissipation effects are negligible in both situations. We shall discuss only this kind of fields. In this frame, some important phenomena involving scalar quantities may be found in the theory of mixing (where Θ is the concentration of a second fluid), and in the study of other transport problems (where Θ is the temperature, the humidity, ...) [M83]. An important example of vectorial quantity advected by the fluid is the vorticity, although it is not of the passive type. The advection by the flow of another vectorial quantity – the magnetic-field intensity – is of great influence in magnetohydrodynamics [W85]. In this section, we are mainly concerned with conserved scalars; the magnetic dynamo is treated in subsect. 4·5.

In the following we focus our attention on incompressible flows for which $\nabla \cdot \boldsymbol{u} = 0$. This means that the volume of an element of fluid, δV, remains

constant along the motion

$$\frac{\mathrm{D}}{\mathrm{D}t}\delta V \equiv (\partial_t + \boldsymbol{u}\cdot\nabla)\,\delta V = 0\,.$$

If $\mathrm{d}\boldsymbol{S}$ represents a (plane) element of a material surface, *viz.* which always contains the same particles of fluid, and $\mathrm{d}\boldsymbol{l}$ a material (straight) line element intersecting $\mathrm{d}\boldsymbol{S}$, the above equation can also be written as

$$\frac{\mathrm{D}}{\mathrm{D}t}(\mathrm{d}\boldsymbol{l}\cdot\mathrm{d}\boldsymbol{S}) = 0\,. \tag{4.1}$$

We shall consider the dispersing fields as being passively convected, *i.e.* we shall disregard their influence on the fluid. According to the definitions, and neglecting molecular diffusion, the evolution laws are

$$(\partial_t + \boldsymbol{u}\cdot\nabla)\,\Theta = 0\,, \tag{4.2}$$

and

$$(\partial_t + \boldsymbol{u}\cdot\nabla)\,(\boldsymbol{F}\cdot\mathrm{d}\boldsymbol{S}) = 0 \tag{4.3}$$

for a scalar and a vector quantity, respectively. Equation (4.2) indicates that the value of the scalar quantity Θ does not change along the motion of fluid particles. Each level surface of Θ follows the evolution of the material surface which is singled out by a particular Θ value. On the other hand, (4.1) and (4.3) show that the vector quantity $\boldsymbol{F}$ is proportional to $\mathrm{d}\boldsymbol{l}$, an infinitesimal line element which initially has the same direction of $\boldsymbol{F}$. The lines of force of $\boldsymbol{F}$ thus follow the evolution of the material lines.

Therefore, as long as the molecular diffusion can be neglected, the changes in the distribution of local quantities, like Θ and $\boldsymbol{F}$, are determined by macroscopic effects related to the behaviour of the solutions of the hydrodynamic equations.

This is a simple consequence of the conservative properties of Θ and $\boldsymbol{F}$. To get some further insight into the behaviour of these fields, one must be able to say something about the Lagragian properties of the flow. It is at this point that we can resort to the experience on Lagrangian chaos (see sect. **2**).

4·1. *The growth of scalar gradients.* – Let us discuss the evolution of the gradients of passive scalars, $\nabla\Theta$, by using concepts borrowed from the theory of dynamical systems.

In Lagrangian terms, the solution of (4.2) is

$$\Theta(\boldsymbol{x},\,t) = \Theta_0(\boldsymbol{T}^{-t}\boldsymbol{x})\,, \tag{4.4}$$

where $\Theta_0(\boldsymbol{x}) \equiv \Theta(\boldsymbol{x},\,0)$ is the initial distribution, and $\boldsymbol{T}^t$ is the operator which gives the evolution $\boldsymbol{x}(t) = \boldsymbol{T}^t\boldsymbol{x}(0)$, related to the equation

$$\dot{\boldsymbol{x}} = \boldsymbol{u}(\boldsymbol{x},\,t). \tag{4.5}$$

One can write the spatial derivative of a passive scalar as

$$\frac{\partial \Theta(\boldsymbol{x}, t)}{\partial x_k} = \sum_{j=1}^{d} \frac{\partial \Theta_0(\boldsymbol{y})}{\partial y_j} \frac{\partial y_j}{\partial x_k}, \tag{4.6}$$

where the variable $\boldsymbol{y} = \boldsymbol{T}^{-1}\boldsymbol{x}$ is given by the time-reversed equation:

$$\dot{\boldsymbol{y}} = -\boldsymbol{u}(\boldsymbol{y}, -t) \qquad \boldsymbol{y}(0) = \boldsymbol{x}. \tag{4.7}$$

The terms $\partial y_j/\partial x_k$ are strictly connected to the instability properties of (4.7). Indeed, after a time t, an uncertainty $\delta\boldsymbol{y}(0)$ on the initial condition becomes

$$\delta\boldsymbol{y}(t) = \tilde{\boldsymbol{A}}(t)\,\delta\boldsymbol{y}(0),$$

where the matrix elements of the linear operator $\tilde{\boldsymbol{A}}$ are $\tilde{A}_{ik} = \partial y_j/\partial x_k$. Then, the behaviour of $|\nabla\Theta|$ is essentially the same of $|\partial\boldsymbol{y}(t)/\delta\boldsymbol{y}(0)|$: if the system (4.5) is chaotic, this is the case also for the solution of (4.7), due to the volume-preserving nature of the dynamics. The global chaotic behaviour is characterized by the maximum Lyapunov exponent of the time-reversed flow

$$\lambda_1 = \lim_{t\to\infty} \frac{1}{t} \ln \left| \frac{\delta\boldsymbol{y}(t)}{\delta\boldsymbol{y}(0)} \right| = \lim_{t\to\infty} \frac{1}{t} \ln |\nabla\Theta|.$$

Therefore, λ_1 gives the typical exponential growth of the gradients.

It is worth stressing that the maximum Lyapunov exponent λ_1 of the reserve motion is equal to the opposite of the minimum Lyapunov exponent of the direct motion. The sum of the Lyapunov exponents is zero for conservative systems (in our context defined by the flows of incompressible fluids). Therefore, the absolute value of the maximum and minimum Lyapunov exponents is always equal in two dimensions. In three dimensions this could be false. It is thus conceivable to find a different value for the maximum Lyapunov exponents of the direct and of the reversed flows, although they seem to be equal in most situations [FKP88]. However, even if in three dimensions the statistics of contractions and expansions were not identical, these arguments should be still valid, since the only important feature is the presence of Lagrangian chaos, *i.e.* $\lambda_1 > 0$ and hence $\lambda_d < 0$ in the direct flow.

4·2. *The multifractal structure for the distribution of scalar gradients.* – The maximum Lyapunov exponent is the typical rate of increasing in the distance of nearby trajectories. Nevertheless, there exist fluctuations around λ_1 of the effective Lyapunov exponent γ computed for a finite time trajectory. In fact, the local growth rate $\gamma(\boldsymbol{x}, t)$ is defined by

$$|\nabla\Theta| \propto \exp[\gamma t] \tag{4.8}$$

and $\lim_{t\to\infty} \gamma(\boldsymbol{x}, t) = \lambda_1$, for almost all initial conditions $\boldsymbol{x}$. The generalized Lyapunov exponents, $L(q)$, are a natural way of characterizing these finite time

fluctuations. They are defined as follows:

$$\overline{|A_{jk}|^q} = \overline{\left|\frac{\partial (\boldsymbol{T}^{-t}\boldsymbol{x})_j}{\partial x_k}\right|^q} \sim \exp[L(q)\,t], \qquad \text{for large } t, \tag{4.9}$$

where $\overline{(...)}$ means time average. The $L(q)$ will be discussed in more details in subsect. **6**·3. The relation between the maximum Lyapunov exponent and $L(q)$ is given by

$$\lambda_1 = \lim_{q\to 0} \frac{L(q)}{q}.$$

From general theorems of probabilty theory [F71], $L(q)$ is shown to be a convex function of q, *i.e.*

$$\frac{L(q')}{q'} \geq \frac{L(q)}{q} \qquad \text{for } q' > q,$$

implying

$$L(q) \geq q\lambda_1 .$$

The equal sign holds only when the effective Lyapunov exponent has negligible finite-time fluctuations $O(1/t)$. In most cases, it is sensible to assume that the probability of measuring a given effective Lyapunov exponent decays as $\exp[-S(\gamma)\,t]$ for $\gamma \neq \lambda_1$. It can be shown that $L(q) = \max_\gamma [\gamma q - S(\gamma)]$, the Legendre tansform of $S(\gamma)$. Gaussian γ-fluctuations (*i.e.* lognormal fluctuations of the gradients) correspond to $S(\gamma) = (\gamma - \lambda_1)^2/(2\sigma^2)$ and $L(q) = \lambda_1 q + (\sigma^2/2)\,q^2$. The absence of γ-fluctuations corresponds to the linear behaviour $L(q) = \lambda_1 q$.

Using (4.6) and (4.9), for the moments of order q we have

$$\langle |\nabla\Theta(\boldsymbol{x}, t)|^q \rangle \sim \exp[L(q)\,t], \tag{4.10}$$

where $\langle ... \rangle$ means spatial average and, if the system is chaotic, we made the ergodic assumption $\overline{(...)} = \langle (...) \rangle$.

Let us consider now the probability measure $\mathrm{d}\mu(\boldsymbol{x}) \propto |\nabla\Theta(\boldsymbol{x})|\,\mathrm{d}\boldsymbol{x}$, and its coarse-graining over boxes Λ_i of size l: $p_i(l) = \int_{\Lambda_i} \mathrm{d}\mu(\boldsymbol{x})$. If one looks at the scaling properties of the moments of the discretized measure with respect to the size of the boxes, one expects $\langle (p_i(l))^q \rangle \propto l^{(q-1)d_q + d}$, where d is the spatial dimension and d_q are the Renyi dimensions [HJKPS86, PV87a]. In the literature the interested reader can find the relations between the generalized dimensions d_q and $L(q)$ [BPTV88]. Here it is sufficient to note that the intermittency in the chaotic behaviour, *i.e.* a nonlinear dependence of L on q, leads to a multifractal structure of the probability measure μ. That is to say, the coarse-grained probability scales with a position-dependent index $p_i(l) \propto l^{\alpha(i)}$, where $\alpha(i)$ is the singularity of the point $\boldsymbol{x}$, centre of the box Λ_i, with respect to the Lebesgue measure, which would give $p_i(l) \propto l^d$. The domi-

nant contribution to the moment of order q is given by an appropriate value $\bar{\alpha}(q)$, that is by the boxes with $\alpha(i) \in [\bar{\alpha}, \bar{\alpha} + \mathrm{d}\alpha]$. The more relevant the multifractality, the larger the deviations of d_q from a constant value, see subsect. **6**·4.

Negleting the diffusion coefficient, the conservative nature of (4.2) implies that the support of the measure μ is the full space, *i.e.* the fractal dimension $d_0 = d$. Moreover, it has been shown for rather generic cases that a nonuniform growth of $\nabla\Theta$ leads to an information dimension (fractal dimension of the set of full probability measure) $d_1 < d_0$, and to an anomalous scaling with a non-constant d_q [PV87a].

Such a multifractal objects is observable only on length scales

$$l > l_2 \sim l_0 \exp[-\gamma_{\max} l], \tag{4.11}$$

where l_0 is the initial scale of $\nabla\Theta$ and $\gamma_{\max}$ is the maximum local growth rate. This is due to the fact that for $l < l_2$, the volume stretching which originates the increase of the Θ gradients, has had no time enough to act. One can also obtain an upper limit for the scale where multifractality can be observed (see subsect. **4**·4, remark IV).

If χ_θ is the appropriate diffusion coefficient, that takes into account the changes in the distribution of Θ due to molecular effect, the molecular diffusion is expected to be effective in smoothing the scalar-field distribution at scale

$$l_d \sim \sqrt{\chi_\theta / \lambda_1}\,. \tag{4.12}$$

Therefore, the approximate equation (4.2) breaks down and has to be replaced by the diffusionlike equation:

$$\frac{\mathrm{D}}{\mathrm{D}t}\Theta = \chi_\theta \nabla^2 \Theta \tag{4.13}$$

after the typical time needed by the stretching mechanism to generate a scale of order l_d, *i.e.* $t_d \sim (1/\lambda_1) \ln (l_0 \sqrt{\lambda_1/\chi_\theta})$. For $t > t_d$, the gradients typically stop their exponential growth. Actually, as the highest γ-value in (4.8) begins to satisfy the relation $\gamma t \sim \ln (l_0 \sqrt{\lambda_1/\chi_\theta})$, a gradual smoothing of the highest gradients should appear with corresponding modifications of the dimension d_q for the q-order moments to which they give the main contribution.

4·3. *The power spectrum of scalar fields.* – We discuss the fluctuations of passive scalars on length scales that are small enough, such that the convected quantity is able to forget its gross scale initial state but not too small, in order to safely neglect the molecular diffusion effects.

Useful information on the small-scale properties of $\Theta(\boldsymbol{x})$ is provided by the structure function [MY75]

$$S_\theta(r) = \langle |\Theta(\boldsymbol{x} + \boldsymbol{r}) - \Theta(\boldsymbol{x})|^2 \rangle = 2 \int_0^\infty \Gamma(k) \left(1 - \frac{\sin kr}{kr}\right) \mathrm{d}k\,, \tag{4.14}$$